Appendix A

THE THERMAL BUILDING SIMULATION MODEL RADCOOL

A.1 SPARK as the Environment for RADCOOL

The Simulation Problem Analysis and Research Kernel (SPARK) is a modular simulation environment that allows the efficient creation of customized models for detailed analysis of building components, systems and subsystems [1-2]. The use of SPARK as the environment for thermal building simulation programs provides three advantages from the point of view of programming.

First, the structural element of SPARK is an object representing a single equation, either algebraic or differential. Larger SPARK elements (macros) can be created based on single equation objects. This provides flexibility, as the user can define new macro objects whenever the need arises. The use of the single equation as a structural object also provides the benefit of code reuse, as the same object can be used in many macro objects without modification.

Second, the structural objects and macro objects are defined in SPARK as mathematical models only, rather than as algorithms. This means that component models do not have a predetermined specification of input or output variables, so variables can be interconnected arbitrarily. In contrast, most of the widely used modular simulators employ algorithmic component models with prescribed input/output relationships. Such models are inherently less flexible, limiting the class of problems that can be defined without modification of the component models.

Third, in SPARK, components are interconnected merely by identifying object interface variables with problem variables (i.e. variable “x” represents a given quantity in one or more equations). Once all equations (objects) are thus interconnected, some variables are specified by the user as the problem inputs, thereby defining a specific problem. The only requirement is that the problem so defined have a solution that is uniquely determined from the specified inputs. Inverting a problem, i.e. changing which variables are inputs and which are outputs, can be done without revising component models or interconnections.

The use of SPARK as the environment for thermal building simulation programs has one main disadvantage: the difficulty of using logical statements. The use of SPARK is appropriate only if there are many interconnections between variables (i.e. the problem to be solved can be described as a large network of simultaneous equations). Logical statements are by nature bound to a sequential approach to solve a given problem. The

use of logical statements in SPARK is cumbersome, will lead to long computation times, and will require large amounts of disk space.

A.2 The Structure of RADCOOL

RADCOOL was created in the SPARK environment in the form of a SPARK building component library, plus a set of user activities. After taking into consideration the benefits and disadvantages of SPARK, RADCOOL was given the following structure:

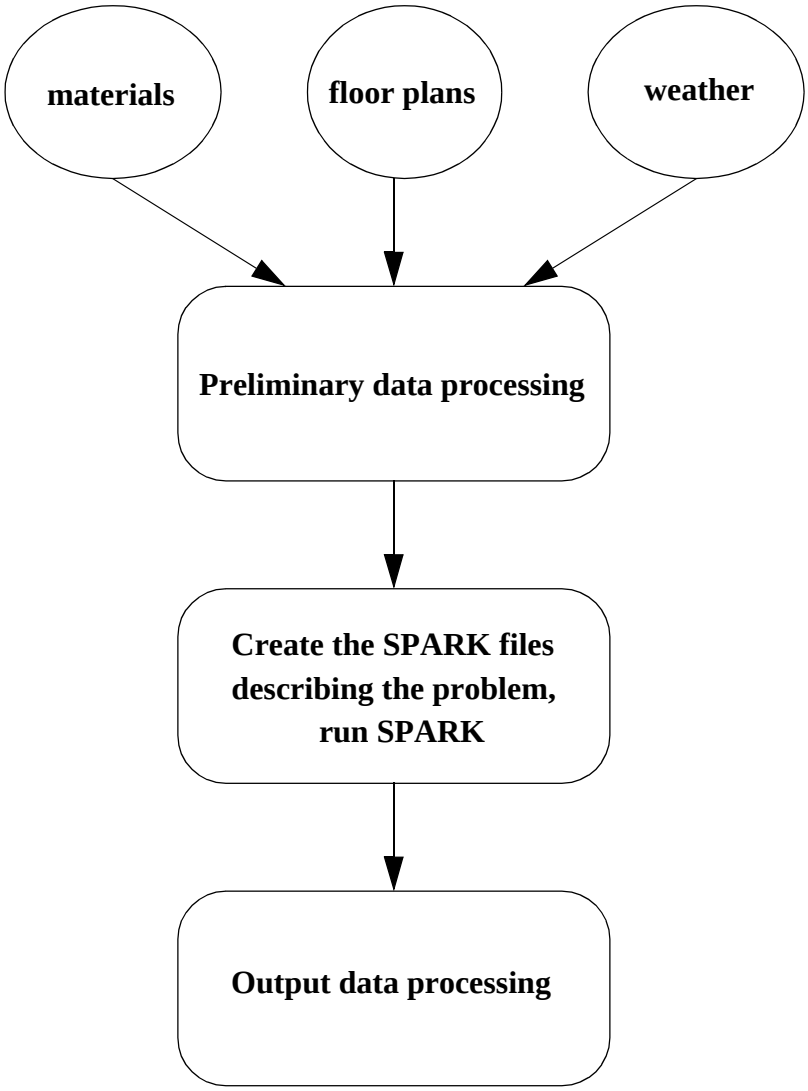

Figure A.1. RADCOOL program flow.

A.2.1 Preliminary data processing

In the “preliminary data processing” section the user gathers data so that a complete description of the simulation problem can be created. This involves obtaining information about building materials, floor plans, internal load schedules, weather data, simulation period, etc. and deciding the length of time steps. In the “preliminary data processing” section the user also performs the calculations necessary to determine shape factors, convection film coefficients, and weather-related variables, because these calculations are not cyclic, so they should not be performed in the SPARK environment.

A.2.2 Create the SPARK files describing the problem, run SPARK

The information acquired in the “preliminary data processing” section provides a unique description of the building to be modeled. Based on this data and using the Network Specification Language, the user creates the files needed for running the building model in SPARK. First, the problem specification (`.ps`) file is created by “assembling” building components from the SPARK component library. Then, based on the user-specified inputs, the constant and dynamic input files are created. The constant input file contains data that does not change with time, such as the thicknesses and thermal properties of building components, building dimensions, shape factors, etc. The dynamic input file contains data that change over time, such as the outdoor air temperature, solar radiation incident on a wall, convection film coefficients, building occupancy, and activity rates.

When all the necessary files have been created, the user runs SPARK. SPARK processes the trio *problem specification file - constant input file - dynamic input file* by creating a C program, compiling it, and executing it. At the end of the simulation the results for each time step are listed in an output file.

A.2.3 Output data processing

In the “output data processing” section the user employs a set of pre-existing programs to display the results of the SPARK simulation in the form of graphs and/or tables. These programs extract and/or plot time-dependent output variables (e.g. air temperature, surface temperatures, water flow rate, water temperature, etc.).

A.3 The SPARK Building Component Library

As described in section A.2, the problem of modeling the thermal behavior of a building in RADCOOL consists of (1) gathering information about the building to be modeled and (2) selecting and “assembling” building components from the SPARK library.

The SPARK building component library contains classes of components. A class of components is defined by its specific properties (e.g. passive or active wall), by the internal links between its sub-classes, and by the links to the other classes of components. The input required for a class reflects the character of the class, and can differ from class to class.

In its present version, RADCOOL has seven classes of components in its SPARK library. The classes are listed below, each class having its corresponding sub-classes attached. The sub-classes are linked together as each class is created.

1. One-dimensional passive four-layer wall with thermal mass.

   a. heat conduction/storage for each of the four layers of the wall.

   b. for exterior walls: radiant heat balance on the exterior surface, including incident solar radiation and long wave radiation exchange with the surroundings.

   c. interior surface radiant heat balance, including infrared and short wave radiation calculations.

2. One-dimensional passive four-layer ground level floor with thermal mass.

   a. heat conduction/storage for each of the four layers of the floor.

   b. exterior heat balance (ground contact).

   c. interior surface radiant heat balance, including infrared and short wave radiation calculations.

3. One-dimensional two-pane window with thermal mass.

   a. heat conduction/storage for each of the two panes.

   b. exterior surface radiant heat balance (for first pane), including calculations of the incident and transmitted solar radiation, and infrared radiation exchange with the surroundings.

   c. interior surface radiant heat balance (for second pane), including infrared and short wave radiation calculations.

4. Two-dimensional active core-cooling ceiling with 5x5 grid structure.

   a. heat conduction/storage for each of the grid cells, and into the water pipes.

   b. heat conduction/storage in the two water regimes (flowing/stagnant).

   c. control strategies for the cooling mode.

   d. for roofs: exterior surface radiant heat balance.

   e. interior surface radiant heat balance.

5. One-dimensional active cooling panel (isothermal panel suspended under a ceiling with thermal mass).

a. heat balance on the top and bottom surfaces of the panel, and heat transfer to the water pipes.

b. heat conduction/storage in the two water regimes (flowing/stagnant).

c. control strategies for the cooling mode.

d. heat conduction/storage and surface balance for the ceiling with thermal mass located above the plenum.

6. Heat and moisture balance for room air (and plenum air, if applicable).

a. room air heat balance.

b. plenum air heat balance.

c. air moisture balance.

7. Linking objects between classes of components.

a. connection between the room air module and the room surfaces (for the modeling of convection heat transfer)

b. connection between the plenum air module and the plenum surfaces, where applicable.

c. interior short wave radiation calculations.

d. interior long wave radiation calculations.

In order to “assemble” a building from components, elements of different classes must be linked together, hence the “linking object” class of components.

Having a single-valued syntax is crucial for this process. In the following, the syntax is the same as that used in the program, which causes a somewhat clumsy appearance of the text and of the equations. However, for better orientation of potential RADCOOL users, readability was given preference over aesthetics.

All variables described in the text have SI units: kilogram [kg], meter [m], second [s] and Kelvin [K], and units derived from these four.

Variable names that start with q or I have units of [W/m^2]. Variable names that start with Q have units of [W]. The names of temperatures start with t, unless in a differential equation involving time, where they start with T.

A.4 The Passive Building Components

A.4.1 One-dimensional heat transfer

A good approximation in the modeling of building components, such as passive walls and windows, is to consider that their surfaces, and all the imaginary internal planes parallel to the surfaces, are isothermal. This approach neglects surface temperature gradients and edge effects. However, the benefits of one-dimensional heat transfer offset the inaccuracies introduced in the results by the isothermal approximation.

A.4.1.1 The one-dimensional heat conduction/storage equation

Consider an infinitely high and wide wall, with homogenous and isotropic material properties, and one-dimensional heat flow perpendicular to the surface of this wall. The temperature at each point over the thickness of the wall can be defined as a space- and time-dependent function, $T = T(x, t)$, where x is the space variable, and t the time variable.

Consider a volume element, ΔV, with heat flux $q(x, t)$ incident on one surface and a heat flux $q(x + \Delta x, t)$ incident on the opposite surface, as shown in Figure A.2.

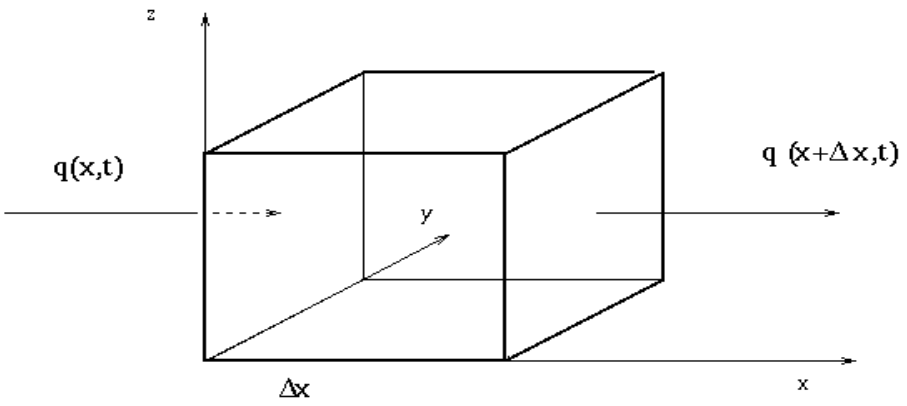

Figure A.2. Volume element for conduction heat flow.

The Fourier equation gives the conduction heat flux as:

$$q(x, t) = -k\frac{\partial}{\partial x}T(x, t) \qquad \text{(A.1)}$$

where

k is the thermal conductivity of the material [W/m-K].

If $\bar{T}(x, t, \Delta t)$ is defined as:

$$\bar{T}(x, t, \Delta t) = \frac{1}{\Delta t} \int_{t}^{t + \Delta t} T(x, \tau) d\tau \tag{A.2}$$

$T_M(x, \Delta x, t)$ as:

$$T_M(x, \Delta x, t) = \frac{1}{\Delta x} \int_{x}^{x + \Delta x} T(\xi, t) d\xi \tag{A.3}$$

and $\bar{q}(x, t, \Delta t)$ as:

$$\bar{q}(x, t, \Delta t) = -k \frac{\partial T(x, t, \Delta t)}{\partial t} \tag{A.4}$$

then the heat balance for the volume element over the time period Δt is:

$$\begin{aligned} &S\Delta t(\bar{q}(x + \Delta x, t, \Delta t) - \bar{q}(x, t, \Delta t)) \\ &+\Delta V \rho c_t (T_M(x, \Delta x, t + \Delta t) - T_M(x, \Delta x, t)) = 0 \end{aligned} \tag{A.5}$$

where:

S is the surface area of the volume element normal to the direction of heat flow [m^2]

ρ is the density of the material [kg/m^3]

c_t is the specific heat of the material [J/kg-K].

Considering equation (A.4), and the relation between the volume and the thickness of the volume element

$$\Delta V = S\Delta x \tag{A.6}$$

the heat balance equation becomes

$$k \left(\frac{\left(\frac{\partial}{\partial x} \bar{T} \right)_{x + \Delta x} - \left(\frac{\partial}{\partial x} \bar{T} \right)_{x}}{\Delta x} \right) = c_t \rho \frac{T_M(x, t + \Delta t) - T_M(x, t)}{\Delta t} \tag{A.7}$$

In the limit $\Delta x \to 0$ and $\Delta t \to 0$, this leads to the heat diffusion equation

$$\frac{\partial T}{\partial t} = \alpha \frac{\partial^2 T}{\partial x^2} \tag{A.8}$$

where α is the thermal diffusivity [m^2/s]:

$$\alpha = \frac{k}{\rho c_t} \tag{A.9}$$

A.4.1.2 The RC approach to solve the heat conduction/storage equation for one solid layer in SPARK

Consider the wall from Section A.4.1.1. Equations (A.1) and (A.8) represent the differential equations for heat conduction through, and heat storage in, the wall. In this section the two equations are simplified and brought into a form that can be easily solved in SPARK. To this end, the space dependence of the temperature must be expressed in finite difference form.

The analogy of the Fourier equation and the heat diffusion equation with Ohm's law and the electrical diffusion equation is obvious. By virtue of this analogy, a "lumped thermal resistance" R_t can be defined as:

$$q = \frac{\Delta T}{R_t} \tag{A.10}$$

and a "lumped thermal capacitance" C_t can be defined as:

$$q = C_t \frac{\partial T}{\partial t}. \tag{A.11}$$

The idea behind the RC approach is to express equations (A.1) and (A.8) by means of (A.10) and (A.11), so that the right-hand side of equation (A.8) can be given a finite difference expression. Comparing (A.10) and a finite difference expression of (A.1), the thermal resistance of a layer of thickness Δx can be defined as

$$R_t = \frac{\Delta x}{k} \tag{A.12}$$

Now comparing (A.8), (A.11) and (A.12), the thermal capacity of a layer of thickness Δx can be defined as

$$C_t = \rho c_t \Delta x \tag{A.13}$$

Using (A.9) in (A.12), (A.13),

$$\alpha = \frac{(\Delta x)^2}{R_t C_t} \tag{A.14}$$

Equations (A.10) - (A.13) give the "lumped RC" model of a homogenous, isotropic wall layer. This model is, however, a crude approximation of the real case, in which each infinitesimal layer dx of the wall can have its own resistance and capacity. To use the RC approach more accurately, a wall must be modeled as composed of a number of layers, each having its own resistance and capacity expressed by equations similar to (A.12) and (A.13), respectively. As the number of layers simulated increases each layer becomes thinner (Δx decreases). In the limit, the RC model approaches the real equations of heat transfer and storage.

A.4.2 The structure of the passive wall in SPARK

Considering that the scope of RADCOOL is to model the thermal performance of buildings, the SPARK module corresponding to the heat conduction/storage sub-component of a wall should be able to handle at least four layers of different materials. To this end, the RC model of each layer was created, then the overall wall component was designed as a system of equations comprising the heat conduction and storage equations for each layer.

Several test programs were written in SPARK to determine the number of sub-layers that must be defined to give good agreement with analytical solutions. The results show that a combination of three resistances and two capacitances (Figure A.3) differs only in the order of a few percent from a combination of four resistances and three capacitances (Figure A.4). However, the computation time increases significantly for the case of four resistances and three capacitances, as compared to the case of three resistances and two capacitances. It was therefore considered appropriate that each layer be modeled as having a maximum of three sub-layers (three resistances and two capacitances).

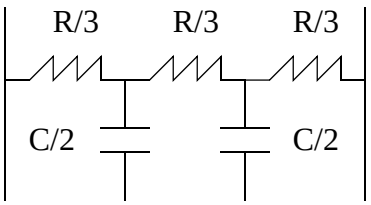

Figure A.3. A wall layer with three sub-layers.

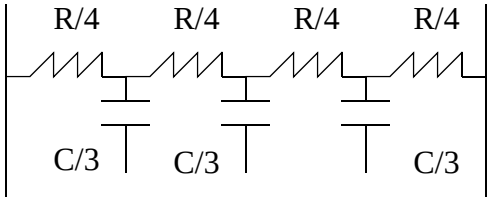

Figure A.4. A wall layer with four sub-layers.

Another important consideration in selecting the final "equivalent circuit" for the wall was that, out of the four wall layers, only the surface layers are exposed to convection, long wave (IR) radiation, and solar radiation (for exterior layer), whereas the two middle layers are not exposed to any sources of radiation. In consequence, in the present version of RADCOOL, each of the two surface layers is modeled as having a structure of three sub-layers, while each of the middle layers is modeled as having a structure of two sub-layers. The equivalent RC circuit is shown in Figure A.5.

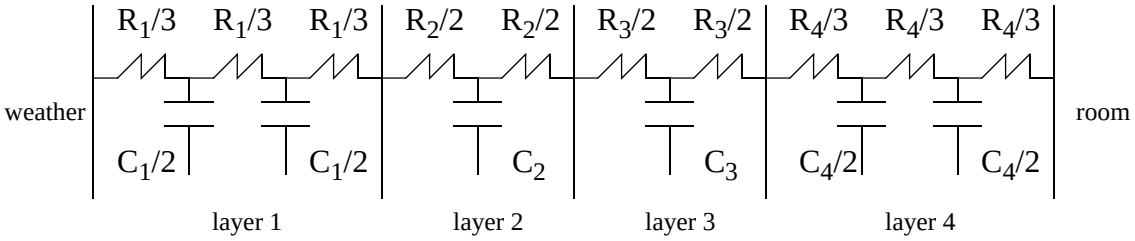

Figure A.5. The RC model of the 4-layer wall.

A.4.2.1 The equations for the temperature nodes in SPARK

The SPARK module that simulates heat conduction/storage in a four-layer passive wall solves the system of equations describing the heat balance at each temperature node. The temperature nodes can be identified from Figure A.5: each surface layer contains two interior temperature nodes, each interior layer contains one interior temperature node, each interface between two layers contains one temperature node, and each wall surface contains one temperature node.

Consider interior node *i*. Denote by *i*-1 and *i*+1 the nodes located immediately adjacent to node *i*. Denote by R_{i-1} and R_{i+1} the resistances of the sub-layers (*i*-1, *i*) and (*i*, *i*+1), and by C_i the capacity corresponding to node *i*. The heat balance equation for node *i* is:

$$\frac{T_{i-1} - T_i}{R_{i-1}} = C_i \frac{dT_i}{dt} + \frac{T_i - T_{i+1}}{R_{i+1}} \tag{A.15}$$

Consider interface node i. Denote by *i*-1 and *i*+1 the nodes located immediately adjacent to node *i*. Denote by R_{i-1} and R_{i+1} the resistances of the sub-layers (*i*-1, *i*) and (*i*, *i*+1). The heat flux balance equation for interface node *i* is:

$$\frac{T_{i-1} - T_i}{R_{i-1}} = \frac{T_i - T_{i+1}}{R_{i+1}} \tag{A.16}$$

Consider wall surface node *i*. Denote by *i*+1 the node locate immediately adjacent, inside the wall. Denote by R_{i+1} the resistances of the sub-layer (*i*, *i*+1), and by q_i the sum of heat fluxes incident on the wall. The heat flux balance equation for the surface node *i* is:

$$q_i = \frac{T_i - T_{i+1}}{R_{i+1}} \tag{A.17}$$

The system of equations for a 4-layer wall with the equivalent circuit shown in Figure A.5 is therefore composed of:

- 6 differential equations of type (A.15), corresponding to the interior nodes,
- 3 algebraic equations of type (A.16), corresponding to the interface nodes, and
- 2 algebraic equations of type (A.17), corresponding to the surface nodes.

A.4.2.2 Test to determine the accuracy of the RC model for one-dimensional heat transfer

In order to determine the accuracy of the RC wall model described in section A.4.2.1 the analytical solution of a given problem was compared with the results from the SPARK model of the same problem.

The problem

Consider the problem of one-dimensional heat transfer in a homogenous and isotropic wall of thickness *l* ($0 < x < l$), with the planes $x = 0$ and $x = l$ kept at temperatures 0 °C and $\sin(\omega t+\varepsilon)$ [°C], respectively [3].

The analytical solution

The temperature of a node at distance x from the plane $x = 0$ is [3]:

$$T(x, t) = A\sin(\omega t + \varepsilon + \phi) + 2\pi\alpha \sum_{n=1}^{\infty} \frac{n(-1)^n(\alpha n^2\pi^2 \sin\varepsilon - \omega l^2 \cos\varepsilon)}{\alpha^2 n^4 \pi^4 + \omega^2 l^4} \sin\frac{n\pi x}{l} e^{-\frac{\alpha n^2 \pi^2 t}{l}} \tag{A.18}$$

where

$$A = \left|\frac{\sinh \mathbf{k}x(1+i)}{\sinh \mathbf{k}l(1+i)}\right| = \left\{\frac{\cosh 2\mathbf{k}x - \cos 2\mathbf{k}x}{\cosh 2\mathbf{k}l - \cos 2\mathbf{k}l}\right\}^{\frac{1}{2}} \tag{A.19}$$

$$\phi = \arg\left\{\frac{\sinh \mathbf{k}x(1+i)}{\sinh \mathbf{k}l(1+i)}\right\} \tag{A.20}$$

and

$$\mathbf{k} = \left(\frac{\omega}{2\alpha}\right)^{\frac{1}{2}} \tag{A.21}$$

The input data

To compare the analytical solution given by equations (A.18) - (A.21) with the results of the SPARK model, a 20 cm concrete wall was modeled and the temperature in the middle of the wall (x = 10 cm) was calculated. The thermal diffusivity was $\alpha = 7.2 \times 10^{-7}$ m^2/s. The sine temperature function at the x = 20 cm surface was chosen to have a period of 24 hours ($\omega = 7.3\ 10^{-5}\ s^{-1}$) and no time lag ($\varepsilon = 0$).

To determine the analytical solution a FORTRAN program was written in which 100,000 terms in (A.18) were summed to calculate the temperature at each time step.

The SPARK program was designed with all four layers having the same thickness (5 cm) and the same thermal properties: density ρ = 2400 kg/m^3, specific heat c_t = 1040 J/kg-K, and conductivity k = 1.8 W/m-K (which gives α = 7.2 10^{-7} m^2/s).

Results

Figure A.6 compares the SPARK result with the analytical solution for the temperature in the middle of the wall (x = 10 cm). The SPARK curve is the result of several iterations. The sinusoidal temperature at the x = 20 cm surface of the wall is also shown. There is good agreement between the SPARK result and the analytical solution of the problem.

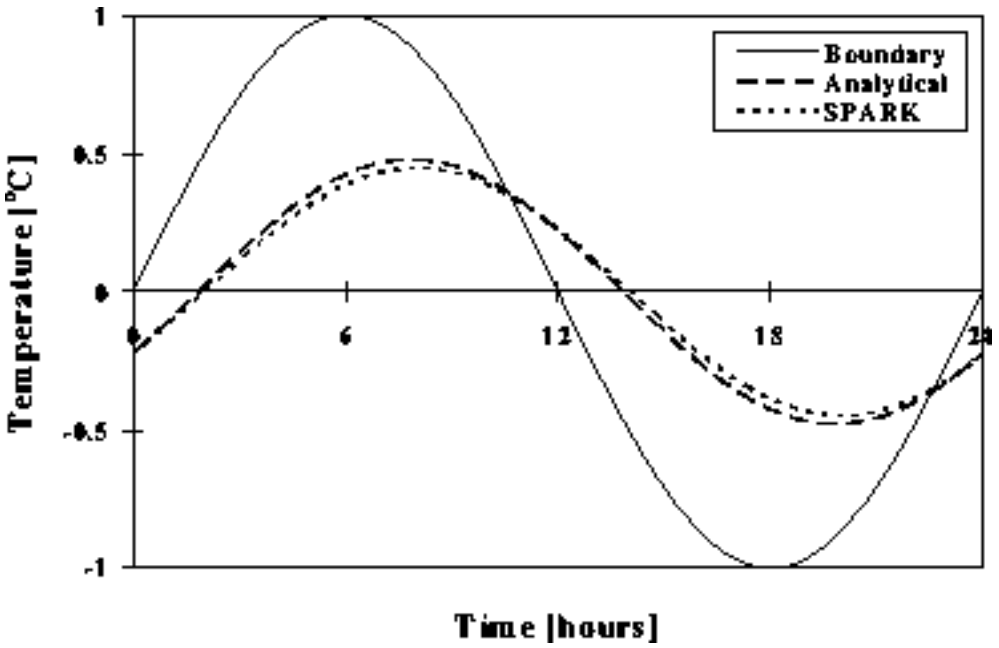

Figure A.6. Temperature at the midpoint of a homogeneous wall: comparison between the one-dimensional SPARK model and the analytical solution.

A.4.3 Exterior surface radiant heat balance for a wall with thermal mass

In this section the radiant heat balance is defined for the exterior (weather-exposed) surface temperature node of a wall (see Figure A.5). The heat fluxes that enter the heat balance equation are shown in Figure A.7.

Heat fluxes into the surface node point are considered positive. All variable names in this object have the suffix *out_obj_i* to emphasize the reference to the exterior surface of the wall number *i*.

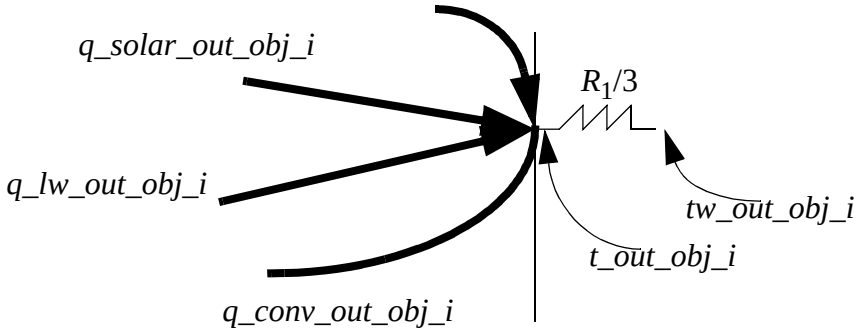

Figure A.7. The heat flux balance at the exterior surface node.

The heat balance is given by:

$$q_{conv-out-obj-i} + q_{lw-out-obj-i} + q_{solar-out-obj-i} = \frac{t_{out-obj-i} - t_{w-out-obj-i}}{\frac{R_1}{3}} \quad \text{(A.22)}$$

where

$q_{conv\_out\_obj\_i}$ is the convective heat flux at the exterior surface of wall *i* [W/m^2]

$q_{lw\_out\_obj\_i}$ is the long wave (IR) heat flux from the surroundings of wall *i* [W/m^2]

$q_{solar\_out\_obj\_i}$ is the solar radiation incident on surface of wall *i* [W/m^2].

The right-hand side of equation (A.22) is the conduction flux through the first exterior sub-layer of wall *i* (refer to equation (A.17) and Figure A.5).

A.4.3.1 The convective heat flux on the surface of a wall

The convective heat flux incident on a surface is defined as the product of the convective film coefficient and the temperature difference between the surface and the air near the

surface:

$$q_{conv} = h_{conv}(t_{air} - t_{surface}) \quad \text{(A.23)}$$

The air temperature near the wall surface and the convective film coefficient usually depend on the location on the surface.

The convective film coefficient of an exterior wall depends on the outside air temperature and on the wind speed and direction. The convective film coefficient of an interior wall depends on the room air temperature and on the air movement (speed and direction). Consequently, this coefficient is not constant for a surface.

In RADCOOL, the air temperature near the exterior wall in equation (A.23) is considered equal to the outside air temperature. In order to use a realistic convective film coefficient in the calculation, hourly values are obtained from a DOE-2 calculation. The model employed by DOE-2 is based on [4].

A.4.3.2 The long wave (IR) heat flux exchange between a wall and its exterior surroundings

The long wave radiation exchange between the exterior surface of a wall and the building surroundings (the ground, sky and atmosphere) is represented in Figure A.8 [5].

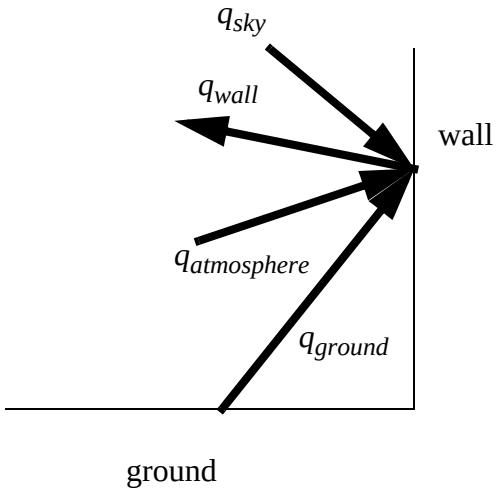

Figure A.8. The long wave radiation exchange at the exterior surface of a wall.

q_{sky} is the long wave radiation from the sky that is absorbed by the wall surface [5]:

$$q_{sky} = \varepsilon_{wall}\sigma\varepsilon_{sky}T_{air}^4 F_{sky}\cos\left(\frac{\Phi_{wall}}{2}\right) \quad \text{(A.24)}$$

where

T_{air} is the ambient air drybulb absolute temperature [K]

ε_{wall} is the wall surface emissivity (equal to 0.9 for most building materials)

ε_{sky} is the effective sky emissivity; it depends on the outside air absolute dew-point temperature T_d, and the cloud cover fraction N:

$$\varepsilon_{sky} = \left(0.787 + 0.76ln(\frac{T_d}{273})\right)(1 + 0.224N - 0.0035N^2 + 0.00028N^3) \quad \text{(A.25)}$$

where

σ is the Stefan-Boltzmann constant (5.67×10^{-8} W/m^2-K^4).

F_{sky} is the sky form factor, defined as the fraction of the hemisphere seen by the wall surface that is subtended by the sky; F_{sky} depends on the tilt of the wall, Φ_{wall} (Φ_{wall} = 90° for a vertical wall, Φ_{wall} = 180° for a floor and Φ_{wall} = 0° for a horizontal roof):

$$F_{sky} = \frac{1 + \cos\Phi_{wall}}{2} \quad \text{(A.26)}$$

$q_{atmosphere}$ is the long wave radiation from the atmosphere that is absorbed by the wall surface [5]:

$$q_{atmosphere} = \varepsilon_{wall}\sigma T_{air}^4 F_{sky}\left(1 - \cos\left(\frac{\Phi_{wall}}{2}\right)\right) \quad \text{(A.27)}$$

q_{ground} is the long wave radiation from the ground absorbed by the wall surface [5]:

$$q_{ground} = \varepsilon_{wall}\sigma\varepsilon_{ground}T_{air}^4 F_{ground} \quad \text{(A.28)}$$

ε_{ground} is the ground emissivity (equal to 0.9)

F_{ground} is the fraction of the hemisphere seen by the wall surface as being subtended by the ground; it is also called ground form factor:

$$F_{ground} = \frac{1 - \cos\Phi_{wall}}{2} \quad \text{(A.29)}$$

For a building that does not have vegetation (trees, bushes) nearby, $F_{ground} + F_{sky} = 1$.

q_{wall} is the long wave radiation emitted by the wall surface:

$$q_{wall} = \varepsilon_{wall}\sigma T_{wall}^4 \quad \text{(A.30)}$$

ε_{wall} is the wall surface emissivity

T_{wall} is the wall surface absolute temperature [K].

The long wave radiation gain on the exterior surface of the wall can be expressed as:

$$q_{lw} = q_{sky} + q_{atmosphere} + q_{ground} - q_{wall} \quad \text{(A.31)}$$

A.4.3.3 The solar radiation incident on the surface of a wall

The solar radiation incident on the exterior surface of a wall has a direct and a diffuse component. The wall absorbs a fraction of each, in amounts dictated by the values of the direct and diffuse absorption coefficients of the wall. The total solar radiation absorbed by the wall is therefore the sum of the absorbed direct and absorbed diffuse solar radiation:

$$q_{solar-out-i} = I_{dir-abs-out-i} + I_{diff-abs-out-i} \quad \text{(A.32)}$$

where

$$I_{dir-abs-out-i} = abs_{dir-oout-i} I_{dir-out-i} \quad \text{(A.33)}$$

$$I_{diff-abs-out-i} = abs_{diff-out-i} I_{diff-out-i} \quad \text{(A.34)}$$

where

$I_{dir\_abs\_out\_i}$ is the portion of the direct solar radiation incident on the exterior surface of wall *i* that is absorbed at the surface [W/m^2]

$abs_{dir\_out\_i}$ is the direct absorption coefficient of wall *i*

$I_{dir\_out\_i}$ is the direct solar radiation incident on the exterior surface of wall *i* [W/m^2]

$I_{diff\_abs\_out\_i}$ is the portion of the diffuse solar radiation incident on the exterior surface of wall *i* that is absorbed at the surface [W/m^2]

$abs_{dir\_out\_}i$ is the diffuse absorption coefficient of wall *i*

$I_{diff\_out\_i}$ is the diffuse solar radiation incident on the exterior surface of wall *i* [W/m^2].

Most building materials have absorptivities of 0.9. The absorptivities of glass surfaces are lower; a typical value for the absorptivity of clear glass is 0.84.

In RADCOOL, the values of the direct and diffuse solar radiation incident on the exterior surface of each wall are requested as inputs. The calculation of these parameters is performed in the "preliminary data processing" section. The calculations will be described in section A.9.2.

A.4.4 Interior surface radiant heat balance for a wall with thermal mass

In this section the radiant heat balance is defined for the interior (room-exposed) surface temperature node of the wall (see Figure A.5). The heat fluxes that enter the heat balance equation are shown in Figure A.9.

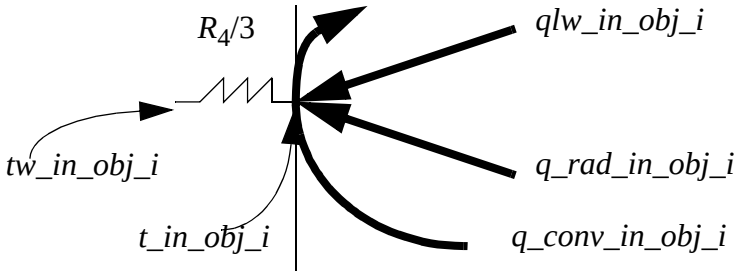

Figure A.9. The heat flux balance at the interior surface temperature node.

Incoming heat fluxes at a node are considered positive. The variable names in this object have the suffix *obj_in_i* to emphasize the reference to the surface of wall *i*. The heat balance is given by:

$$q_{conv-in-obj-i} + q_{lw-in-obj-i} + q_{rad-in-obj-i} = \frac{t_{in-obj-i} - t_{w-in-obj-i}}{\frac{R_4}{3}} \quad \text{(A.35)}$$

where

$q_{conv\_in\_obj\_i}$ is the convective heat flux at the interior surface of wall *i* [W/m^2]

$q_{lw\_in\_obj\_i}$ is the net long wave (IR) radiation flux gain from the radiative exchange between the wall *i* and the other walls in the room [W/m^2]

$q_{rad\_in\_obj\_i}$ is the radiation incident at the interior surface of wall *i* from the sources inside the room (people, equipment and lights), and from the solar radiation entering the room through transparent surfaces [W/m^2].

The right-hand side of equation (A.35) represents the conduction flux through the first interior sub-layer of wall *i* (refer to equation (A.17) and Figure A.5).

A.4.4.1 The convective heat flux on the interior surface of a wall

The convective heat flux on the interior surface of the wall is given by equation (A.23).

In most applications the room air temperature and the convective heat coefficient can be averaged over the surface. For example, Figure A.10 shows the surface temperature of a vertical wall and the air temperature near the surface as a function of height. At the "neutral level" both temperatures are the same. The direction of the heat flux is from the wall towards the air at locations under the "neutral level", and from the air to the wall at locations above the "neutral level." In order to simulate each wall surface represented by only one node, an expression for the convection film coefficient at this one node must be found that reflects the variation of this coefficient over the wall surface.

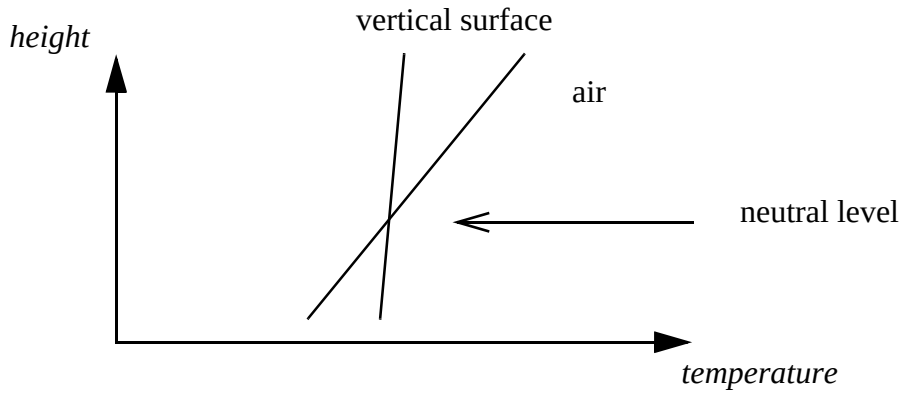

Figure A.10. Different gradients for air and room temperatures.

The interior convective film coefficient, *h_conv_in_i*, depends on the properties of the air, the wall surface roughness, and the air movement near the wall. There are several levels of simplification for calculating this variable.

- constant value: as a first approximation, *h_conv_in_i* may be assumed constant. Building simulation programs employ values in the range from 1 to 3.5 W/m^2-K [6].

- a function of temperature difference between the surface and the air near the surface; there are several such expressions (see [7] for example):

$$h_{conv-in-i} = C_1(\Delta t)^{C_2} \qquad \text{(A.36)}$$

where C_1 and C_2 are considered constant, or depend on the properties of the air and of those of the surface.

- a function of the physical properties of the air and the surface; calculating the convective film coefficient based on this method is based on determining air flow patterns near the surface.

Considering the limitations of SPARK, in RADCOOL the interior convective film coefficient is considered constant and equal to the value employed in DOE-2 (3.25 W/m^2-K).

A.4.4.2 The long wave radiative exchange between a wall and the other room surfaces

Consider an enclosure composed of *N* discrete surfaces, each having a determined temperature T_i. A complex long wave (IR) radiative exchange occurs inside the enclosure as radiation is emitted by a surface, travels to the other surfaces, is partly reflected and re-reflected many times within the enclosure, with partial absorption at each contact with a surface.

There are several approaches for the calculation of the net long wave flux gain by a surface as a result of this radiative exchange inside the enclosure. The two approaches that are adequate for a building simulation program are the *mean radiant temperature* approach and the *net-radiation* approach. RADCOOL uses the net-radiation approach.

The mean radiant temperature approach

This approach approximates that the interaction between a given wall and the rest of the surfaces in the enclosure can be described as the interaction between two surface elements. The equation governing the radiative exchange is the grey body equation for two surface elements, one at the temperature of the wall, and the other at the mean radiant temperature. The mean radiant temperature is defined as the temperature of a half sphere that causes a net heat flux on the wall equal to the heat flux caused by the real enclosure.

Considering that all the walls forming the enclosure have the same emissivity, the net long wave radiation on surface number *i* can be expressed as

$$q_{long-wave-in-i} = \varepsilon_{in-i}\varepsilon_{sphere-in-i}\alpha_{rad-in-i}(T_{MRT-in-i} - T_{in-i}) \qquad \text{(A.37)}$$

where

$T_{MRT\_in\_i}$ is the mean radiant temperature of the enclosure with respect to surface *i* [K]

T_in_i is the temperature of surface *i* [K]

ε_{in_i} is the emissivity of surface *i* [-]

$\varepsilon_{sphere\_in\_i}$ is the weighed average of the emissivities of the other surfaces [-]

$\alpha_{rad\_in\_i}$ is the radiative heat transfer coefficient defined in analogy to the convective heat transfer coefficient [W/m^2-K].

Consider an "enclosure" consisting of two infinitely long and wide walls facing each other. If the two walls can be represented as black bodies, the radiative heat exchange between them can be written as:

$$q_{12} = \sigma(T_1^4 - T_2^4) = \alpha_{rad-in-i}(T_1 - T_2) \qquad \text{(A.38)}$$

with

$$\alpha_{rad-in-i} = \sigma(T_1^3 + T_1^2 T_2 + T_1 T_2^2 + T_2^3) \qquad \text{(A.39)}$$

where σ is the Stefan-Boltzmann constant (equal to 5.67x10^{-8} W/m^2-K^4). $\alpha_{rad\_in\_i}$ is equal to 5 - 7 W/m^2-K over the temperature range occurring in buildings.

Raber and Hutchinson [8] mention the influence of reflectance, and state that the reflectance may be neglected if emissivities are higher than 0.9. Assuming that $\alpha_{rad\_in\_i}$ is the same for all pairs of walls, Raber and Hutchinson derive:

$$T_{MRT-in-i} = F_{i1}T_1 + F_{i2}T_2 + \ldots + F_{ij}T_j \qquad \text{(A.40)}$$

where

T_i,...,T_j are the temperatures of the surfaces of the enclosure

F_{ij} is the shape factor of surface *i* to surface *j*, equal to the fraction of the long wave radiation emitted by surface *i* that is absorbed by surface *j*.

The calculation of the shape factors is relatively simple in the case of flat surfaces (see [9]), but rather complicated in the case of rounded surfaces. Section A.9.3 will present the calculation method used to determine the shape factors in the "preliminary data processing" section of RADCOOL.

The net-radiation approach

The net-radiation approach [9] provides a method to calculate the net (equilibrium) radiation incident on each surface of the enclosure. This approach does not impose any

approximations regarding the types of surfaces in an enclosure, such as a range of emissivities over which equation (A.40) holds, and it therefore suits RADCOOL better than the mean radiant temperature approach.

Consider the area A_i of the enclosure. If q^i_{out} and q^i_{in} are the radiant flux leaving from surface *i*, and incident on surface *i*, respectively, a flux balance at the surface can be written as:

$$q^i_{net} = q^i_{in} - q^i_{out} \tag{A.41}$$

where

$$q^i_{out} = \varepsilon_{in-i}\sigma T^4_{in-i} + (1-\varepsilon_{in-i})q^i_{in} \tag{A.42}$$

Since the incoming radiant flux is a combination of outgoing radiant flux from the other surfaces, an additional equation can be written:

$$q^i_{in} = \sum_{j=1}^{N} F_{ij} q^j_{out} \tag{A.43}$$

By solving the system of equations (A.41) - (A.43), the net radiant gain for each surface can be determined.

A.4.4.3 Solar and internal radiation incident on the interior surface of a wall

Two other sources of radiation on the interior surface of a wall are the short wave (solar) radiation entering the window and the heat radiated by occupants and equipment.

Short wave radiation in a space

In a typical building, short wave solar radiation enters a space through windows and other transparent surfaces (transparent walls, skylights, etc.). This radiation is incident on the different surfaces in the space, according to the position of the windows with respect to the sun, and of the surfaces with respect to the windows. A thorough calculation of this effect would determine the position of the sun at each moment, and, based on the position of the windows in the space, the fraction of the solar radiation entering the space that is incident on each surface. This calculation is not only time consuming, but also needs a follow-up in which the multiple reflections between the different surfaces are determined.

To avoid lengthy calculations and complicated distribution functions for the transmitted

solar radiation, the RADCOOL user performs solar calculations in the "preliminary data processing" section. These calculations (see section A.9.2 for details) determine the solar radiation incident on each building envelope surface, as well as the fractions of the total solar radiation entering the space at each moment.

RADCOOL adopted the DOE-2 approach, in which a given combination of surfaces inside the space receives a certain fraction of the total radiation entering the space. Assuming that each surface in a given combination receives the same amount of radiation per unit area, the incident short wave radiation on each surface can be calculated as:

$$q_{short-wave-in-i} = fraction_{in-i} \frac{\sum_{windows} A_{window-j} q_{short-wave-window-j}}{A_{surfaces-in-i}} \quad \text{(A.44)}$$

q_short_wave_window_j is the amount of solar radiation entering the space through window *i* [W/m^2]

A_window_j is the area of window *i* through which *q_short_wave_window_j* solar radiation enters the space [m^2]

A_surfaces_in_i is the area of the combination of walls including wall *i*, that receives *fraction_in_i* of the total solar radiation entering the space [m^2]

fraction_in_i is the fraction of the total short wave radiation entering the room that is incident on the combination of walls having the total area *A_surfaces_in_i* [-]

q_short_wave_in_i is the amount of solar radiation entering the space that is incident on the combination of walls having the area *A_surfaces_in_i*, including wall *i* [W/m^2].

Occupants and equipment inside a space

The occupants and equipment (including lights) in a space are internal heat sources. In RADCOOL the occupants and equipment are considered to be grey bodies that participate in the long wave radiation exchange in the space (see section A.4.4.2), and sources of sensible and latent heat for the heat and moisture balances in the room air module (see section A.7).

A.4.5 The four-layer passive floor with thermal mass

A.4.5.1 Comparison between the floor and the wall with thermal mass

The main difference between a ground-level floor and an exterior vertical wall is that, while the exterior surface of the floor is in contact with the ground, the exterior surface of a vertical wall is in contact with the outside air, and is exposed to solar radiation.

The exterior surface of a floor therefore participates in conductive heat exchange with the ground, but is not subject to convective or radiative heat exchange. Based on these considerations, the case of a floor can easily be modeled starting with the model of the vertical wall:

• the heat conduction/storage for the four-layer floor with thermal mass is the same as for the four-layer wall with thermal mass (see section A.4.2),

• the interior surface radiant heat balance of a floor is the same as that for a vertical wall (see section A.4.4), and

• the heat balance for the exterior surface node of a floor contains only conduction terms.

A.4.5.2 The exterior surface radiant heat balance for a passive floor with thermal mass

The heat balance for the exterior surface of a floor describes the contact between the floor and the ground. The equivalent of equation (A.17) for this case is

$$q_{ground-out-i} = \frac{t_{out-obj-i} - t_{w-out-obj-i}}{\frac{R_1}{3}} \quad \text{(A.45)}$$

In RADCOOL a resistance is modeled between the floor and the ground temperature nodes. The heat flux incident on the exterior surface of the floor can be calculated as:

$$q_{gound-out-i} = \frac{t_{ground-out} - t_{out-obj-i}}{R_{floor-ground-obj-i}} \quad \text{(A.46)}$$

where

$R_{floor\_ground\_obj\_i}$ is the floor-ground resistance [m^2-K/W]

t_ground_out is the ground temperature [°C]

t_out_obj_i is the temperature of the exterior surface of the floor number *i* [°C].

A.4.6 The two-pane window with thermal mass

A.4.6.1 Comparison between a two-pane window and a multi-layer wall

With the exception of solar radiation effects, a multi-pane window behaves like a multi-layer wall in which one or more of the layers are air (or a different gas). If a temperature difference is created between two window surfaces, or if thermal radiation is directed on one window pane, the glass will undergo heat conduction and storage.

A glass pane and a wall layer have different thermal behavior due to the numerical values of their thermal properties. In a wall layer, the conduction and storage heat transfer are both important, resulting in a significant temperature difference between the two boundaries (surfaces) of the wall layer. In a window pane, the temperature difference between the two surfaces of the glass is small because of the high conductivity of the glass. As glass window panes are usually thin (3 - 6 mm), their thermal storage is also small. However, in a multi-pane window, the overall temperature difference across the window can be significant, especially if the glass has low emissivity coating, and/or the "gap" spaces are filled with a low-conductivity gas.

A.4.6.2 Heat conduction/storage for a two-pane window

The SPARK model for a two-pane window was designed based on the thermal properties of glass. Because of the high conductivity and low heat capacity of a glass pane, a model of one resistance and one capacity was adopted for each pane. A resistance was added between the panes to account for the thermal resistance of the gas fill. Figure A.11 shows the RC model for a two-pane window.

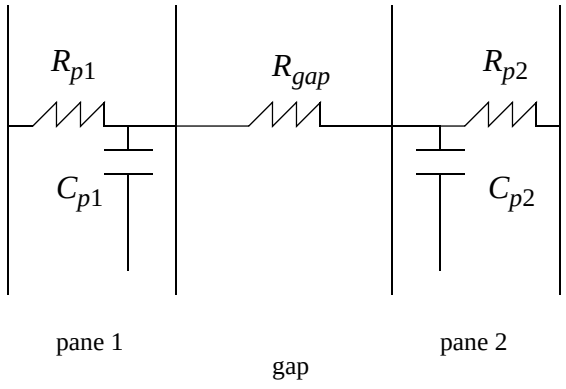

Figure A.11. The RC circuit of a two-pane window.

Two temperature nodes were modeled for each of the two panes, one on the exterior surface and one on the surface facing the "gap".

The equations that describe the heat balance for the two panes are the following:

• for the exterior (weather-exposed) temperature node, the equivalent of equation (A.17) with R_{p1} instead of $R_1/3$ gives

$$q_{rad-out} = \frac{T_{w1,\,out} - T_{w1,\,gap}}{R_{p1}} \tag{A.47}$$

where

q_{rad_out} is the overall radiative heat incident on the exterior pane [W/m^2]

$T_{w1,out}$ is the temperature at the exterior node of the exterior pane [°C]

$T_{w1,gap}$ is the temperature at the "gap"-facing node of the exterior pane [°C]

R_{p1} is the thermal resistance of the exterior pane [m^2-K/W].

• for the gap-exposed temperature node of the exterior pane:

$$\frac{T_{w1,\,out} - T_{w1,\,gap}}{R_{p1}} + C_{p1}\frac{\partial T_{w1,\,gap}}{\partial t} = \frac{T_{w1,\,gap} - T_{w2,\,gap}}{R_{gap}} \tag{A.48}$$

where

C_{p1} is the thermal capacity of the exterior pane [J/m^2-K]

R_{gap} is the thermal resistance of the gas filling the "gap" [m^2-K/W]; it is calculated for each type of window to include thermal diffusion and convection effects

$T_{w2,\,\mathrm{gap}}$ is the temperature at the "gap"-facing node of the interior pane [°C].

• for the gap-exposed temperature node of the interior pane:

$$\frac{T_{w1,\,gap} - T_{w2,\,gap}}{R_{gap}} = C_{p2}\frac{\partial T_{w2}}{\partial t} + \frac{T_{w2,\,gap} - T_{w2,\,in}}{R_{p2}} \tag{A.49}$$

where

C_{p2} is the thermal capacity of the interior pane [J/m^2-K]

R_{p2} is the thermal resistance of the interior pane [m^2-K/W]

$T_{w2,in}$ is the inside temperature at the interior node of the interior pane [°C].

• for the interior (room-exposed) temperature node, the equivalent of equation (A.17), with R_{p2} instead of $R_4/3$ gives

$$\frac{T_{w2,\,gap} - T_{w2,\,in}}{R_{p2}} = q_{rad} \qquad \text{(A.50)}$$

where

q_{rad} is the total incident radiation on the interior pane [W/m^2].

The notation q_{rad} was chosen for the right-hand side of equation (A.50), rather than $q_{\_rad\_in}$, to emphasize that the heat balance for the second pane of a window also includes a fraction of the solar radiation transmitted by the first pane.

A.4.6.3 The heat balance for the exterior pane of a two-pane window

The heat balance for the exterior pane of a two-pane window is the same as that for the exterior surface of a wall. The equation that applies is:

$$q_{conv-out} + q_{lw-out} + q_{solar-1} = q_{rad-out} \qquad \text{(A.51)}$$

The left-hand terms of equation (A.51) are calculated as in sections A.4.3.1 through A.4.3.3.

A.4.6.4 The heat balance for the interior pane of a two-pane window

The heat balance for the interior pane of a two-pane window is similar to that of a wall, except that the solar radiation transmitted through the first pane also contributes to the balance. The transmitted solar radiation calculated in this module will contribute to the overall short wave radiation inside the space. The heat balance equation is:

$$q_{conv-in} + q_{lw-in} + q_{rad-in} + q_{solar-2} = q_{rad} \qquad \text{(A.52)}$$

The first three terms in the left-hand side of equation (A.52) are calculated as in sections A.4.4.1 through A.4.4.3.The last left-hand term is calculated as in section A.4.3.3, with the absorption coefficients corresponding to the overall coefficients for the solar radiation transmitted by the exterior pane.

The solar radiation transmitted through the two-pane window is calculated using the DOE-2 method. If the overall transmissivity coefficients are calculated for the window as a whole, the radiation transmitted through the window is:

$$q_{solar-interior} = I_{trans-dir-win-i} + I_{trans-diff-win-i} \qquad \text{(A.53)}$$

and

$$I_{trans-dir-win-i} = trans_{dir-win-i} I_{dir-out-win-i} \quad \text{(A.54)}$$

$$I_{trans-diff-win-i} = trans_{diff-win-i} I_{diff-out-win-i} \quad \text{(A.55)}$$

where

$I_{dir\_out\_win\_i}$ is the direct solar radiation incident on exterior surface of window *i* [W/m^2]

$I_{diff\_out\ win\_i}$ is the diffuse solar radiation incident on the exterior surface of window *i* [W/m^2].

$I_{trans\_dir\_win\_i}$ is the portion of the direct solar radiation incident on the window *i* that is transmitted through the window [W/m^2]

$I_{trans\_diff\_win\_i}$ is the portion of the diffuse solar radiation incident on the window *i* that is transmitted through the window [W/m^2]

$trans_{dir\_win\_i}$ is the overall transmission coefficient of window *i* in direct solar radiation

$trans_{diff\_win\_i}$ is the overall transmission coefficient of window *i* in diffuse solar radiation.

In order to perform RADCOOL calculations, hourly values for the glass transmission coefficients are obtained from a DOE-2 calculation.

After calculations are performed with equations (A.53) - (A.55) for all the windows of a space, the short wave radiation inside the space can be calculated as:

$$q_{short-wave-tot-in} = \sum_i I_{trans-win-i} \quad \text{(A.56)}$$

A.5 The Active Building Components

A.5.1 Two-dimensional heat transfer analysis

The one-dimensional heat transfer approximation presented in Section A.4.1 does not yield good results in the case of building components incorporating a heat source or sink (e.g. a core-cooling ceiling). Modeling the thermal behavior of such building components requires the use of two-dimensional heat transfer analysis. Two-dimensional heat transfer analysis describes the temperature variation of the given building component in two “main directions” of heat flow (usually the two directions of a cross-section through the building component).

A.5.1.1 The two-dimensional heat conduction/storage equations

Consider a solid ceiling with homogeneous and isotropic material properties. The two-dimensional heat transfer analysis is based on the assumption that the temperature of this ceiling is a function of only two dimensions of the ceiling, and is constant in the third dimension (e.g. the temperature varies over the cross-section of the ceiling, but all the planes parallel to the cross-section under study have the same thermal behavior).

In analogy with Section A.4.1.1, the temperature in the cross-section of a wall can be considered a function of space and time, $T = T(x, y, t)$.

Consider a volume element of this wall slab, and a heat flux incident at one surface, as in Figure A.2. The 2-D Fourier equation for heat transfer in one direction is analogous to equation (A.1) and has the form

$$Q(x, t) = -k\Delta A\frac{\partial T(x, y, t)}{\partial x} \tag{A.57}$$

where

Q is the total heat flux at the surface [W]

k is the thermal conductivity of the ceiling material [W/m-K]

ΔA is the area of the face of the volume element normal to the heat flux [m^2].

The same type of reasoning as in Section A.4.1.1 yields a two-dimensional diffusion equation of the form

$$\frac{\partial T}{\partial t} = \alpha\left(\frac{\partial^2 T}{\partial x^2} + \frac{\partial^2 T}{\partial y^2}\right) \tag{A.58}$$

where

α is the thermal diffusivity given by equation (A.9) [m^2/s].

A.5.1.2 The RC solution to the two-dimensional heat conduction/storage equations

The approach of Section A.4.1.2 can be used to express equation (A.58) as a finite difference equation. The two-dimensional ceiling can be described as a collection of parallel boxes, with the discretization (the grid) covering a plane normal to the surface of the ceiling. Since this discretization is mainly performed to describe the heat transfer due to the presence of cooling pipes inside the ceiling, the assumption was made that the analysis of a “cross-section sample” can correctly describe the temperature profile of the whole ceiling. Consequently, the parallel boxes have one dimension equal to a fraction of the thickness of the ceiling, a second dimension equal to a fraction of the (future) dis-

tance between two cooling pipes, and the third dimension equal to the length of the ceiling divided by the distance between two cooling pipes. The remainder of this section discusses the heat transfer inside a passive two-dimensional ceiling. Section A.5.2 will describe the modeling of the actively cooled two-dimensional ceiling.

In an analogy to electrical circuits, a lumped thermal resistance can be defined in relation to the heat conduction through each box in a given direction, as:

$$Q_\xi = \frac{\Delta T_\xi}{R_\xi} \tag{A.59}$$

where ξ denotes a direction in the three-dimensional space. Similarly, a lumped thermal capacity can be defined in relation to the heat stored inside each box, as:

$$Q = C\frac{\partial T}{\partial t} \tag{A.60}$$

The resistance and capacity are calculated by the thermal properties of the ceiling material as:

$$R_\xi = \frac{\Delta \xi}{k \Delta A_\xi} \tag{A.61}$$

$$C = \rho c_t \Delta V \tag{A.62}$$

where

ΔA_ξ is the area of the box surface normal to the direction ξ [m^2]

ΔV is the box volume [m^3]

ρ is the density of the ceiling material [kg/m^3]

c_t is the specific heat of the ceiling material [J/kg-K]

k is the conductivity of the ceiling material [W/m-K].

A.5.1.3 The two-dimensional model of the ceiling in SPARK

SPARK programs were written to simulate several grids covering the sample section of the ceiling. Figures A.12 and A.13 show two alternative RC circuits, the one in Figure A.13 displaying a “finer” grid structure than the one in Figure A.12.

In the grid model in Figure A.12, the boxes have one dimension equal to a third of the ceiling thickness, and a second dimension equal to a quarter of the distance between the

cooling pipes. In the grid model in Figure A.13, the boxes have one dimension equal to a fifth of the ceiling thickness, and a second dimension equal to a quarter of the distance between the cooling pipes.

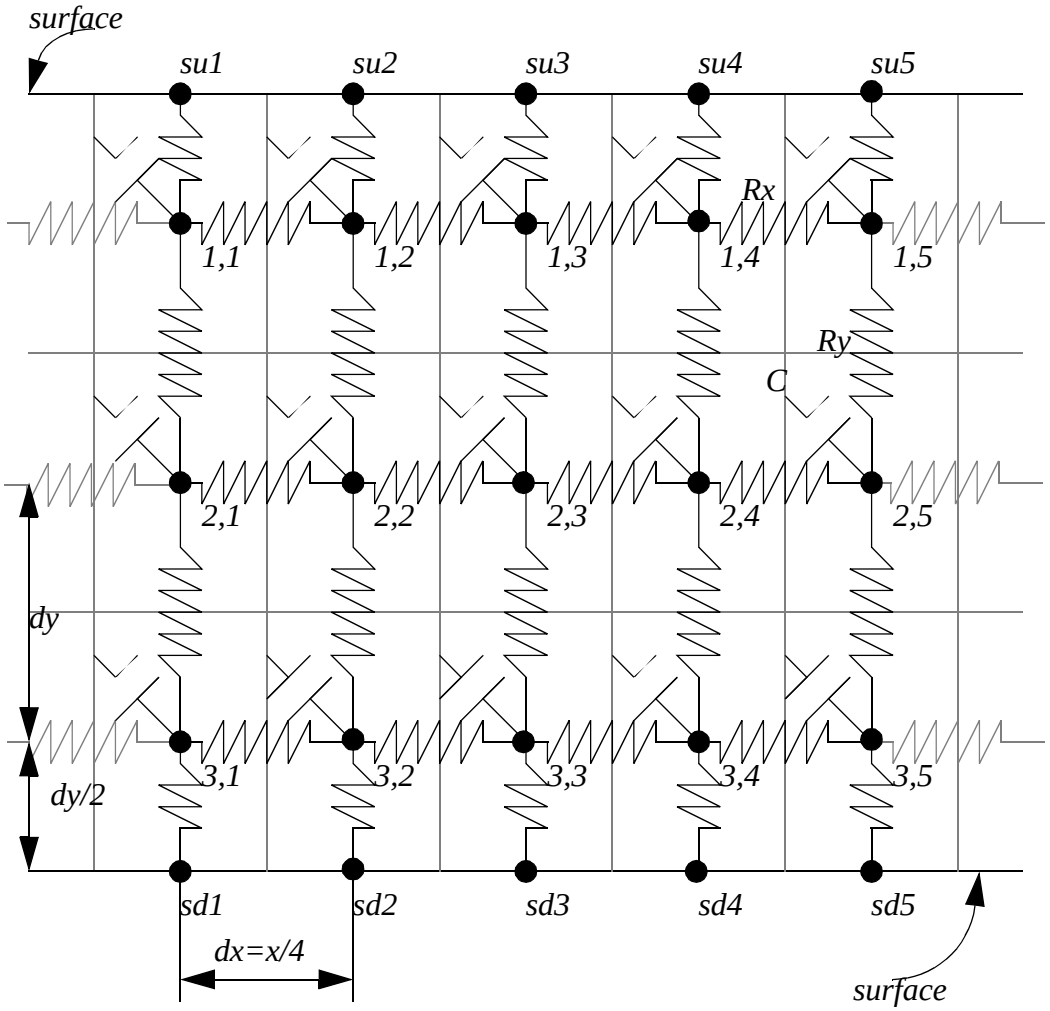

Figure A.12. A 3 x 5 grid. RC equivalent circuit for heat transfer calculations.

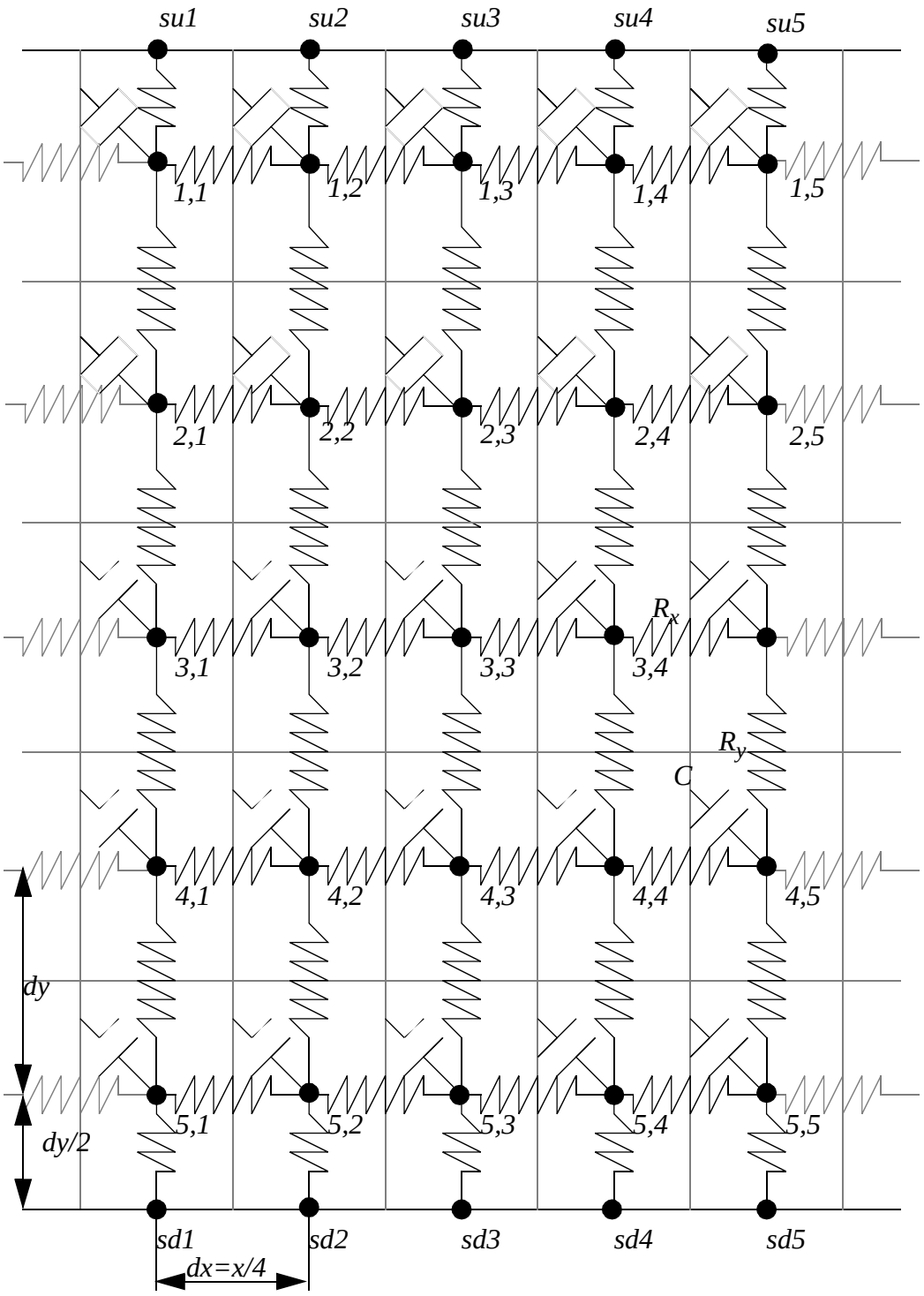

Figure A.13. A 5 x 5 grid. RC equivalent circuit for heat transfer calculations.

The resistances and capacitances in Figures A.12 and A.13 are calculated as

$$R_x = \frac{dx}{kdydz} \tag{A.63}$$

$$R_y = \frac{dy}{kdxdz} \tag{A.64}$$

$$C = \rho c_t \Delta V \tag{A.65}$$

and

$$dx = \frac{distance-between-pipes}{n_x} \tag{A.66}$$

$$dy = \frac{thickness-of-wall}{n_y} \tag{A.67}$$

$$\Delta V = dxdy \times z \tag{A.68}$$

where $dz = z$ is the length of the ceiling. For the case in Figure A.12, the number of "cells" in the x direction is $n_x = 4$, and the number of cells in the y direction is $n_y = 3$. For the case in Figure A.13, $n_x = 4$ and $n_y = 5$.

Note. The discretization over the cross-section of the ceiling is not set rigidly in the SPARK model. While the "box thicknesses", *dx*, are always calculated with (A.66), the "box heights", *dy*, can be input by the user to reflect the structure of the ceiling. *dy* can be different for each box layer, and can represent the thicknesses of the different material layers in the ceiling.

The heat balance at the temperature nodes can be derived by analogy with the one-dimensional situation (equations (A.15)-(A.17)). The heat balance for the interior node (*i*,*j*) is

$$\frac{T_{i-1,j} - T_{i,j}}{R_{x,i-1}} + \frac{T_{i,j-1} - T_{i,j}}{R_{y,j-1}} = C_i \frac{dT_{i,j}}{dt} + \frac{T_{i,j} - T_{i+1,j}}{R_{x,i+1}} + \frac{T_{i,j} - T_{i,j+1}}{R_{y,j+1}} \tag{A.69}$$

where

$T_{i,j}$ is the temperature at node (*i*,*j*)

$R_{x,k}$ and $R_{y,k}$ are thermal resistances connecting the node (*i*,*j*) with the rest of the network, in the *x* and *y* directions, respectively [W/K]

C_i is the capacitance of a cell in row *i* [J/K].

The heat balance for a surface node (i,j) is:

$$Q_{i,j} = \frac{T_{i,j-1} - T_{i,j}}{R_{y,j-1}} \qquad \text{(A.70)}$$

where

$Q_{i,j}$ is the total heat flux at the surface [W].

A.5.1.4 Test to determine the accuracy of the RC model for two-dimensional heat transfer

The same problem as in Section A.4.2.2 was simulated for the two grid models. The results from the two-dimensional model with the dimensions dx = 2.5 cm, dy = 4 cm and z = 10 m agree with the analytical solution (see Figures A.14 for the results of the 3x5 grid model and A.15 for the results of the 5x5 grid model).

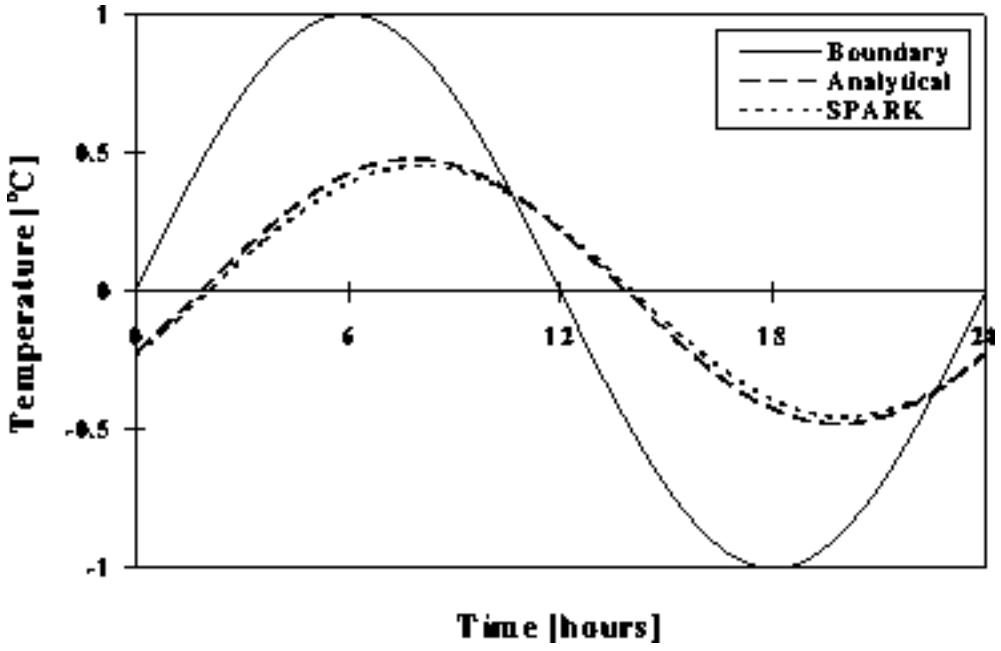

Figure A.14. Temperature at the midpoint of a homogeneous ceiling: comparison between the 3x5 grid SPARK model and the analytical solution.

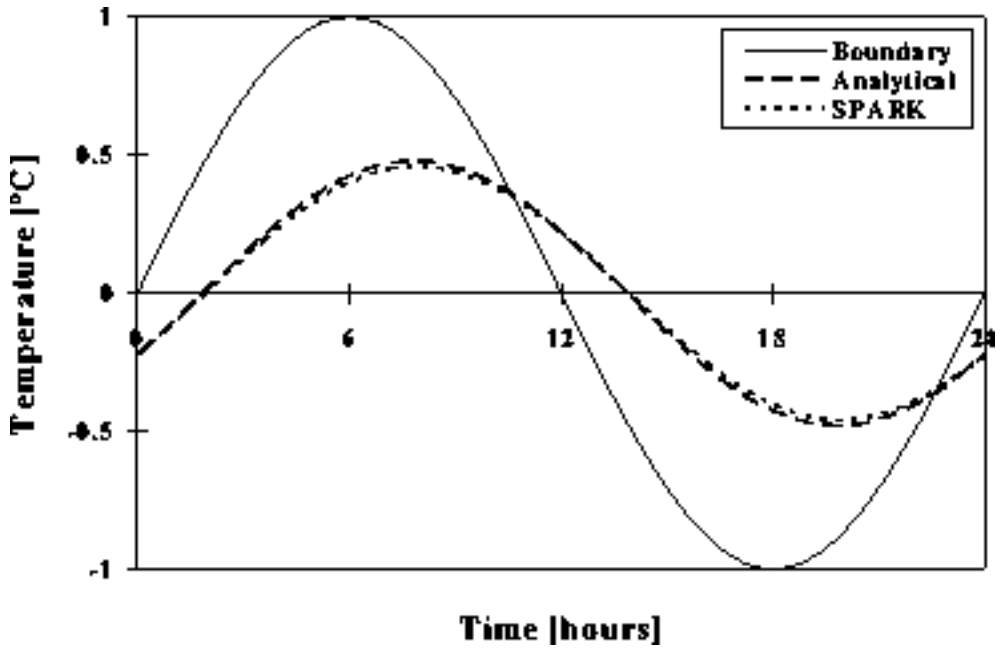

Figure A.15. Temperature at the midpoint of a homogeneous ceiling: comparison between the 5x5 grid SPARK model and the analytical solution.

A.5.2 The two-dimensional SPARK model of the core cooling ceiling

A core cooling ceiling consists of a layer of parallel pipes imbedded in concrete or plaster. Figure A.16 shows the structure of a core cooling ceiling with imbedded pipes.

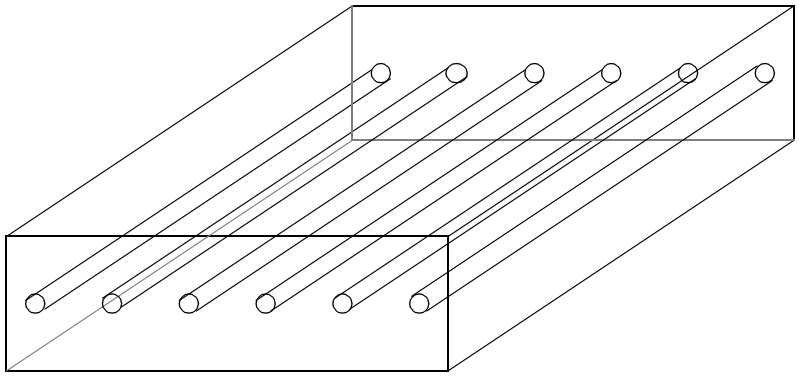

Figure A.16. Structure of a cooled ceiling with imbedded pipes.

The model of a passive two-dimensional ceiling can be easily adapted to reflect the heat transfer through the active core cooling ceiling by declaring the heat transfer between a given pipe and its adjacent grid box as a boundary condition on the grid box.

A.5.2.1 Heat transfer between the pipe and the water when the water is flowing

Consider a water pipe at a given temperature. If water is circulated through the pipe, and if the water temperature is different from the temperature of the pipe, heat is transferred between the pipe and the water. The heat transfer can be expressed as:

$$Q_{convected-water} = hA(T_{pipe} - T_{water-average}) \quad \text{(A.71)}$$

where

h is the convection heat transfer coefficient [W/m^2-K]

A is the total surface area for the heat transfer [m^2]

T_{pipe} is the pipe temperature [°C]

$T_{water\_average}$ is the bulk temperature of the water, defined as the well mixed temperature of the water in the pipe [°C]

$Q_{convected\_water}$ is the heat transferred from the pipe into the water [W].

The convection heat transfer coefficient can be expressed in terms of the fluid and flow characteristics as follows [10]:

$$h = \frac{k}{d}Nu \quad \text{(A.72)}$$

where

k is the conductivity of the fluid [W/m-K]

d is the pipe diameter [m]

Nu is the Nusselt number for the flow [-].

In the case of fully developed turbulent flow in a smooth pipe, the Nusselt number has the following empirical expression [10]-[11]:

$$Nu = 0.023Re^{0.8}Pr^{n} \quad \text{(A.73)}$$

where

Re is the Reynolds number for the flow [-], calculated as

$$Re = \frac{4}{\pi} \frac{\dot{m}}{\mu d} \tag{A.74}$$

and

$\dot{m}$ is the mass flow of the water inside the pipe[kg/s]

μ is the dynamic viscosity of the water [kg/m-s]

d is the pipe diameter [m]

Pr is the Prandtl number of the water [-]

n = 0.4 if the water is heated by forced convection, and n = 0.3 if the water is cooled by forced convection [12].

The heat convected from the pipe is stored in the water, therefore

$$Q_{stored-water} = \dot{m}_{water} c_{water} (T_{return} - T_{inlet}) \tag{A.75}$$

where

c_{water} is the specific heat of water [J/kg-K]

T_{inlet} is the inlet water temperature

T_{return} is the return water temperature

Q_{stored_water} is the heat stored in the water as a result of the heat transfer [W].

The bulk temperature of the water in equation (A.71) can be calculated as

$$T_{water-average} = \frac{T_{return} - T_{inlet}}{2} \tag{A.76}$$

A.5.2.2 Heat transfer between the pipe and the water when the water is recirculated

In order to provide comfort inside a room cooled by radiant cooling, the cooling system must have some control system. Depending on the inlet water temperature, the thermal mass of the ceiling, and the room loads, circulating the water without interruption might cool the room too much, making it uncomfortable. However, if the water flow is discontinued, or if the temperature of the inlet water is raised, the room will not be cooled as fast, and the chances of creating discomfort are reduced.

When the heat transfer between the room and the water accounts for only a small fraction of the cooling power, water recirculation represents a convenient way in which the

cooling system can adjust its output to meet the room cooling loads. The cold water from the chiller is mixed with warmer return water, with the obvious result that the inlet ceiling water temperature becomes higher than that of the cold water supplied by the chiller. The recirculation of water also provides a way to save chiller power.

Consider that two quantities of water m_{cold} and m_{warm}, at different temperatures T_{low} and T_{high}, are mixed together. This process will result in a quantity of water $m_{total} = m_{cold} + m_{warm}$, with a temperature T_{mix} given by

$$m_{warm} c_{water} (T_{high} - T_{mix}) = m_{cold} c_{water} (T_{mix} - T_{low}) \tag{A.77}$$

where c_{water} is the specific heat of water. The temperature of the water after the mixing process is

$$t_{mix} = \frac{m_{cold} t_{low} + m_{warm} t_{high}}{m_{total}} \tag{A.78}$$

or,

$$t_{mix} = x t_{low} + (1 - x) t_{high} \tag{A.79}$$

with the "mixing ratio" expressed as $x = \frac{m_{cold}}{m_{total}}$

In the case where water is mixed from two water streams, $\dot{m}_{total} = \dot{m}_{cold} + \dot{m}_{warm}$ and

$x = \frac{\dot{m}_{cold}}{\dot{m}_{total}}$.

In the case of a cooled ceiling, the two water streams represent cold water from the chiller and warmer return water. The quantity that is constant is the water flow through the ceiling. In this situation, the mass flows corresponding to the cold and warm water streams must be adjusted to the room conditions at each moment.

The most efficient to make the adjustment is based on knowing the response of the room to a change in inlet water temperature. This type of calibration curve provides a relationship between a given room air temperature and the inlet water temperature which must be supplied in order to remove the room loads. However, extensive measurements are necessary in order to determine the calibration curve. An alternative is to substitute the calibration curve with the "opening characteristic" method, which is not as efficient as the calibration curve method, but is more intuitive and requires less financial investment.

Consider a given room air temperature range that provides occupant comfort. The low end, T_{low_end}, of this range can be then made to correspond to the temperature at which the cooling ceiling starts to function, and the high end, T_{high_end} to a temperature at and above which only unmixed cold water is circulating through the ceiling. The mixing ratio is determined in this case as follows:

- when the room air temperature falls below T_{low_end} a "water switch" stops the water flow; the mixing ratio is zero.

- for room air temperatures above T_{high_end} only cold water is circulated; the mixing ratio is 1.

- for room temperatures between T_{low_end} and T_{high_end} a mixture of cold water and warm return water is circulated; the mixing ratio is between 0 and 1.

In general, if the room air temperature is known and the opening characteristic is linear between T_{low_end} and T_{high_end}, the formula expressing the mixing ratio is:

$$x = \frac{T - T_{low-end}}{T_{high-end} - T_{low-end}} \tag{A.80}$$

where T is equal to

- T_{low_end} if $T_{room\_air} < T_{low\_end}$
- T_{room_air} if $T_{low\_end} < T_{room\_air} < T_{high\_end}$
- T_{high_end} if $T_{room\_air} > T_{high\_end}$.

A.5.2.3 Heat transfer between the pipe and the water when the water is stagnant

In the case when the water flow is discontinued, heat from the ceiling is conducted through the pipe and stored in the stagnant water. The heat conducted from the pipe to the stagnant water can be written as

$$Q_{conducted-water} = U_{pipe-water}(T_{pipe} - T_{water-average}) \tag{A.81}$$

where

$U_{pipe\text{-}water}$ is the heat transfer coefficient between the pipe and the water [W/K]

T_{pipe} is the pipe temperature [°C]

$T_{water\_average}$ is the average temperature of the water [°C].

The heat conducted from the pipe into the water warms the water:

$$Q_{stored-water} = m_{water} c_{water} \frac{\partial T_{water-average}}{\partial t} \quad \text{(A.82)}$$

where

$m_{water} = \rho_{water} V_{pipe}$ is the mass of the water inside the pipe.

A.5.2.4 The two-dimensional model of a cooled ceiling

The theoretical model from section A.5.1.3 can be applied to determine the heat transfer between a cooled ceiling and its surroundings. Figure A.13 shows the 5x5 grid of a RC circuit in which each horizontal layer can have a different material structure. The nodes *vj_i,i*+1 are interface nodes between two layers. Only vertical heat flow is modeled at the interfaces, so the heat balance for node *vj_i,i*+1 is

$$\frac{T_{i-1,j} - T_{vj-i-1,i}}{\frac{R_{y,i-1,j}}{2}} = \frac{T_{vj-i-1,i} - T_{i,j}}{\frac{R_{y,i,j}}{2}} \quad \text{(A.83)}$$

where

$R_{y,i,j}$ is the vertical thermal resistance on column *j* and in row *i*.

To model the thermal contact between the ceiling nodes and the water, the exterior of the pipe is considered as having the same temperature as the adjacent ceiling node, while the interior of the pipe is considered as having a temperature equal to the average temperature of the water. Between these two nodes an additional horizontal resistance is introduced, to model the thermal resistance of the pipe itself (see Figure A.17). The additional resistance is a function of the conductivity of the pipe material and reflects the cylindrical symmetry of the pipes:

$$R_{x-pipe-water} = \frac{ln\left(\frac{d_{outside-pipe}}{d_{inside-pipe}}\right)}{2\pi z k_{pipe}} \quad \text{(A.84)}$$

where

$d_{outside\_pipe}$ is the outside diameter of the cooling pipe [m]

d_{inside_pipe} is the inside diameter of the cooling pipe [m]

z is the total length of the pipe [m]

k_{pipe} is the conductivity of the pipe material [W/m-K].

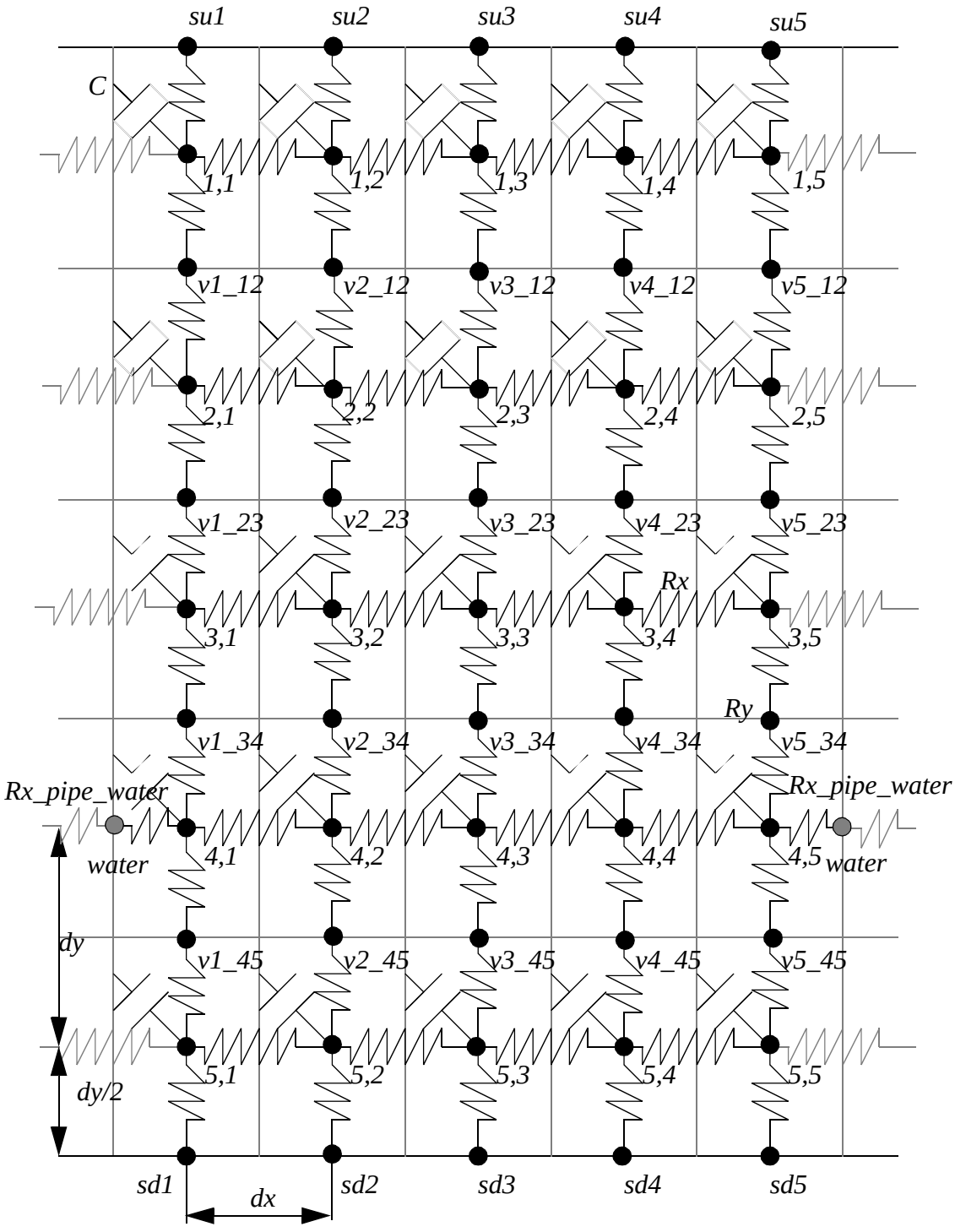

Figure A.17. Equivalent RC circuit for heat transfer calculation in the case of a cooled ceiling.

When the water is flowing, the heat balance at the pipe surface is

$$Q_{conducted-pipe} = Q_{convected-water} = Q_{stored-water} \quad \text{(A.85)}$$

where

$$Q_{conducted-pipe} = \frac{T_{wall-node} - T_{pipe}}{R_{x-pipe-water}} \quad \text{(A.86)}$$

$Q_{convected\_water}$ is given by equation (A.71)

Q_{stored_water} is given by equation (A.75).

In the case where the water flow is zero, the heat balance at the pipe surface is:

$$Q_{conducted-pipe} = Q_{convected-water} = Q_{stored-water} \quad \text{(A.87)}$$

where

$Q_{conducted\_water}$ is given by equation (A.81)

Q_{stored_water} is given by equation (A.82).

A.5.3 The cooling panel

A different type of radiant cooling system is the cooling panel system. This system is consists of aluminum panels with metal pipes connected to the rear of the panel. When cold water is circulated through the pipes a good thermal contact between the pipes and the panel provides very low resistance to heat conduction. As a result, the surface temperature of the panel is virtually equal to the water temperature. For a given room air temperature, the panel surface can be maintained cold by circulating water through the pipes at a given rate. This system is more efficient than the core cooling system because it can respond virtually instantly to a change in room loads.

A.5.3.1 The model of the cooling panel

Cooling panel heat transfer

Consider a room with a cooling panel system. Figure A.18 shows the placement of the different components.

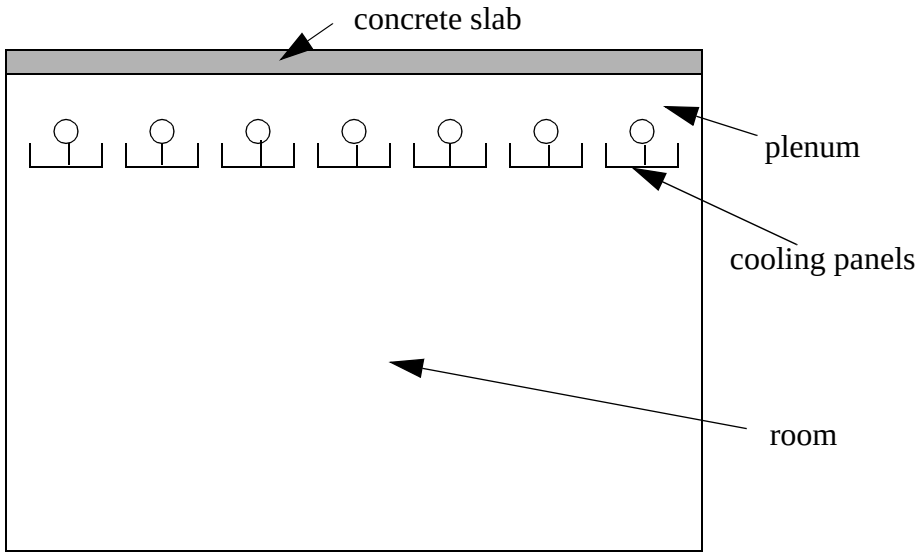

Figure A.18. Layout of a cooling panel system.

The cooling panel exchanges radiation with the other surfaces in the room and with the concrete slab above the plenum. As a result, the room walls, floor, and the plenum slab are cooled. These surfaces will therefore absorb long wave radiation from sources inside the room and will cool the room air by convection. An additional cooling effect is achieved when there is heat exchange between the room air and the plenum air by means of air flow through the interstices between two adjacent panels. In this case, warm room air will rise, will penetrate in the plenum, and will mix with the cooler plenum air.

Heat balance for the cooling panel

Figure A.19 shows the overall heat balance for the cooling panel.

The balance equations are

$$sum-fluxes-room = conv-flux-room + q-lw-room + q-sw-room \quad \text{(A.88)}$$

$$sum-fluxes-plenum = conv-flux-plenum + q-lw-surf-plenum \quad \text{(A.89)}$$

$$cond-flux-panel-pipe = sum-fluxes-room + sum-fluxes-plenum \quad \text{(A.90)}$$

where

conv_flux_room is the convective flux on the room side of the panel [W/m^2]

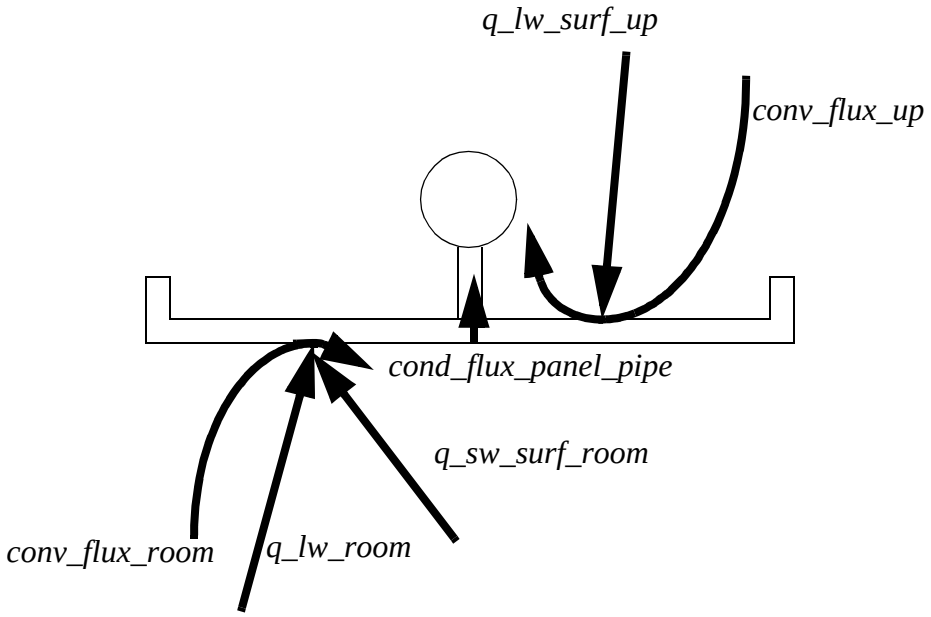

Figure A.19. The heat balance in the case of the cooling panel.

q_lw_room is the long wave flux on the room side of the panel [W/m^2]

q_sw_room is the short wave flux on the room side of the panel [W/m^2]

sum_fluxes_room is the overall flux on the room side of the panel [W/m^2]

conv_flux_plenum is the convective flux on the plenum side of the panel [W/m^2]

q_lw_flux_plenum is the long wave flux on the plenum side of the panel [W/m^2]

sum_fluxes_plenum is the overall flux on the plenum side of the panel [W/m^2]

cond_heat_panel_pipe is the conductive heat flux from the panel to the pipe [W/m^2].

The heat transfer from the pipe to the water is given by

$$Q - cond - pipe - water \; = \; A\text{–}panel \times cond - heat - pane - pipe \qquad \text{(A.91)}$$

where

Q_cond_pipe_water is the heat conducted into the water [W]

A_panel is the area of the panel [m^2].

The mechanisms by which the heat conducted into the water is removed are the same as those for the concrete core cooling (see sections A.5.2.1 - A.5.2.3).

A.6 Types of Radiant Cooling System Controls

As stated in section A.5.2.2, it is possible to maintain comfort conditions inside a room conditioned by radiant cooling by controlling the water flow in the cooled ceiling. However, core cooling systems have a long heat transfer time constant, and the response of the radiant surface temperature to a change in water temperature and/or water flow is relatively slow. In such a case, a control mechanism is needed that allows the occupant to modify the response of the radiant system to specific building loads. This section presents three mechanisms that are used to control the output of existing radiant cooling systems.

A.6.1 The thermostat-based control

The most common type of control for any air-conditioning system is the thermostat-based control. The air temperature inside the room or inside the return plenum is measured. When the loads cause the temperature to rise above a pre-determined setpoint, cooling is started. When the room temperature drops below the setpoint, cooling is stopped.

In the case of radiant cooling systems, the thermostat-based control is used to start or to stop the flow of cold water (see Figure A.20). The thermostat-based control can be represented by the following algorithm:

$$\dot{m}_{water} = \dot{m}_{design} \text{ if } t_{room-air} \geq t_{setpoint}$$

$$\dot{m}_{water} = 0 \text{ if } t_{room-air} < t_{setpoint} \tag{A.92}$$

The advantage of the thermostat-based control consists of its easy implementation. Its main disadvantage is that it cannot address the problem of the delay of the radiant surface response to a change in the system. The thermostat-based control is therefore more suitable for cooling panel systems. Because a cooling panel system has low thermal mass, it can respond quickly to a change dictated by a thermostat-based control system.

A.6.2 The timer-based control

Another type of control is the timer-based control that causes the cooling system to function according to a pre-determined schedule. Figure A.21 shows a schematic of timer-based control.

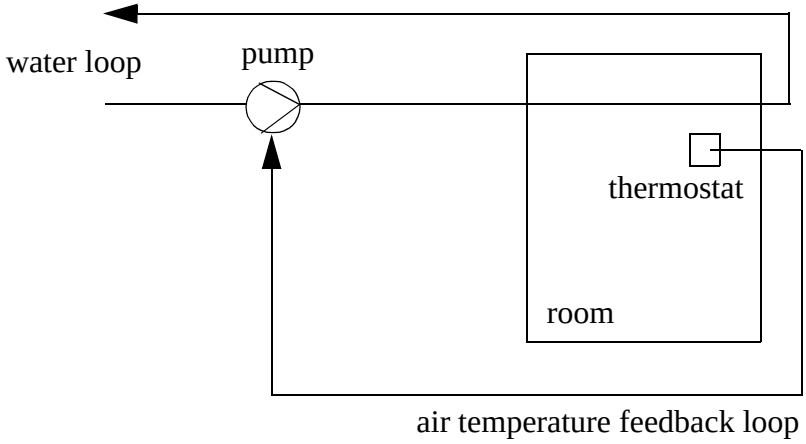

Figure A.20. Thermostat-based control strategy.

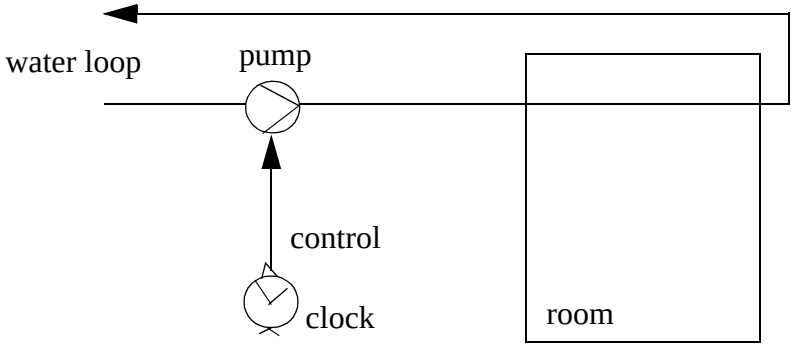

Figure A.21. Timer-based control strategy.

When the response of the building to weather-induced loads and internal loads is known, and the timer-control is done according to this response, the building peak load can be shifted away from its “natural” time of occurrence. For example, if the cooling is done overnight, the time of occurrence of the peak load can be shifted to the evening hours, or even night-time hours.

The timer-based strategy will not, however, respond to rapidly-occurring loads. This observation leads to the conclusion that the timer-based strategy is appropriate only for

certain building types (those with large thermal mass) and certain climates (those with daily temperature amplitudes that are stable over a long period of time).

A.6.3 The hybrid control

The hybrid control is based on the idea of varying the water flow and/or inlet water temperature according to some predetermined information about the cooling system. If the room response to a given change in the operation of the cooling system is known, the system can be operated to "adapt" to the cooling load. If the response of the room is not known, an "opening characteristic" can be used instead (see section A.5.2.2).

One type of a hybrid control strategy for a radiant cooling system is based on adjusting the water inlet temperature to the room load. This control strategy can be achieved by using water recirculation. The ratio of recirculated to total flow is controlled by the room conditions. The schematic of this control strategy is shown in Figure A.22.

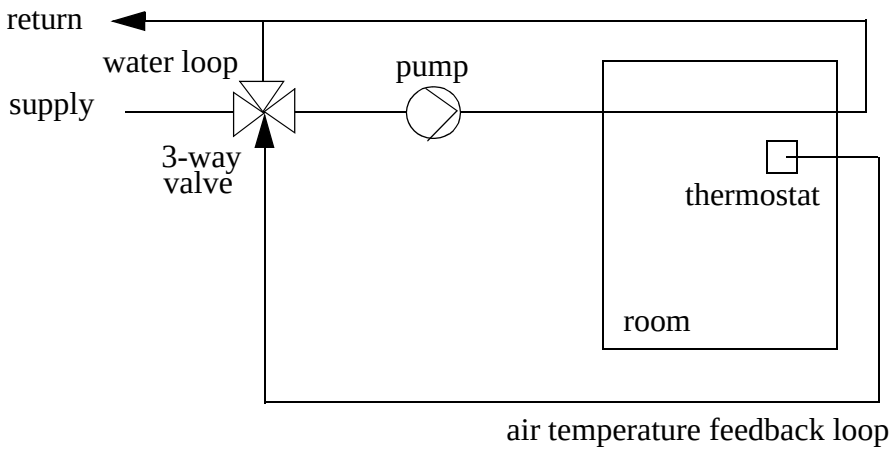

Figure A.22. Hybrid control.

The hybrid control system used in the RADCOOL simulations in Chapter 3 is based on the following formulas:

$$\dot{m}_{inlet} = \dot{m}_{cold} + \dot{m}_{return} \text{ and } T_{inlet} = \frac{\dot{m}_{cold}T_{cold} + \dot{m}_{return}T_{return}}{\dot{m}_{inlet}}$$

where

if $T_{room-air} < T_{setpoint-low}$ then the water flow is stopped, and $\dot{m}_{inlet} = 0$,

If $T_{room-air} \geq T_{setpoint-low}$ then the water flows in the pipes,

$\dot{m}_{cold} = x\dot{m}_{inlet}$, $\dot{m}_{return} = (1-x)\dot{m}_{inlet}$, and

$$x = max\left[\frac{T_{room-air} - T_{setpoint-low}}{T_{setpoint-high} - T_{setpoint-low}}, 1\right].$$

In RADCOOL, the temperature interval [$T_{setpoint\text{-}low}$, $T_{setpoint\text{-}high}$] is required as input.

A.7 The Indoor Air

A.7.1 The air temperature

The indoor air temperature is a function that depends on a large number of parameters. Time, the location inside a space, the thermal properties of air, the nature of the contact between the air and the room envelope surfaces, the presence of an active cooling system, the presence of a ventilation system, space occupancy, and equipment schedules are a few of these parameters. Assuming that the thermal properties of air and the air pressure are constant at any given moment, the room air temperature can be expressed as a function of time and position:

$$T_{air} = T_{air}(x, y, z, t) \tag{A.93}$$

Determining the space-time function for the air temperature is a complicated task. Because of the dependence of the room air temperature on a large number parameters, it is difficult to find a closed form for T_{air}. However, approximate solutions for the air temperature at discrete points can be found.

One way to obtain approximate solutions for the air temperature is to discretize the air domain inside a space and to calculate the mass and heat flows between the subdomains. This procedure constitutes the object of computational fluid dynamics, and is extremely time consuming. Considering the purpose of RADCOOL, it is clear that the interest is not so much in knowing the air temperature at a large number of nodes inside a space, as it is in determining the air temperature at a few points of interest. The “interesting” air temperature points inside a room ar shown in Figure A.23.

The air temperatures shown in Figure A.23 are the following:

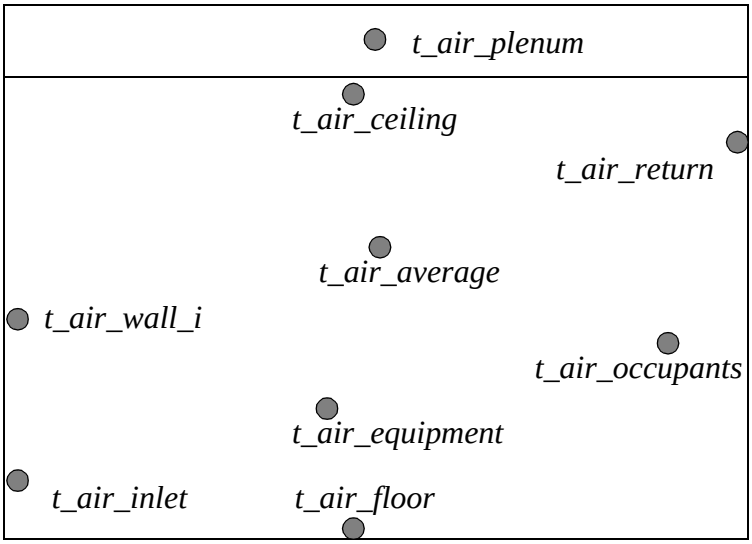

Figure A.23. Air temperatures nodes in a room modeled by RADCOOL.

t_air_inlet is the temperature of the supply air

t_air_average is the air temperature in a room with fully mixed air

t_air_return is the temperature of the air exhausted from the room

t_air_wall_i is the air temperature near wall *i*

t_air_floor is the air temperature near the floor

t_air_ceiling is the air temperature near the ceiling

t_air_occupants is the air temperature near any occupants

t_air_equipment is the air temperature near the equipment

t_air_plenum is the air temperature inside the plenum.

A.7.2 Discretization of the room air domain in RADCOOL

In order to discretize the room air domain some assumptions pertaining to the different air temperatures are necessary. In RADCOOL, each air temperature is expressed as a sum of the temperature of the well-mixed air temperature and a temperature increment:

$$t_{air-wall-i} = t_{air-average} + t_{increment-wall-i} \quad \text{(A.94)}$$

$$t_{air-floor} = t_{air-average} + t_{increment-floor} \quad \text{(A.95)}$$

$$t_{air-ceiling} = t_{air-average} + t_{increment-ceiling} \quad \text{(A.96)}$$

$$t_{air-occupants} = t_{air-average} + t_{increment-occupants} \quad \text{(A.97)}$$

$$t_{air-equipment} = t_{air-average} + t_{increment-equipment} \quad \text{(A.98)}$$

where *t_increment_...* may be constant, or proportional to the cooling load (see [13]).

In the current version of RADCOOL all the increments are input by the user.

The SPARK calculation of the well-mixed air temperature inside a room is based on heat and moisture balances.

A.7.3 Room air heat balance

The air inside a room exchanges heat with the surfaces in the room envelope (walls and windows), and with people and equipment. The air inside a room can also be heated or cooled by the air that infiltrates, and by the air supplied to the room by the ventilation system. If the room is connected to a plenum, the air inside the room can also be cooled through interaction with the plenum air, if the plenum is cooler than the room.

The heat balance for the room air is described in Figure A.24.

The heat balance corresponding to Figure A.24 is:

$$Q_{cap-air} + Q_{conv-in-tot} = Q_{vent-air-room} + Q_{infil-air-room} - Q_{from-room} + Q_{people} + Q_{equipment} \quad \text{(A.99)}$$

where

Q_cap_air is the heat stored in the room air as a result of the heat transfer [W]

Q_conv_in_tot is the total convective heat generated by lights and equipment and lost to the room envelope [W]

Q_vent_air_room is the heat brought into the room by the ventilation system [W]

Q_infil_air_room is the heat brought into the room by air infiltration [W]

Q_conv_from_room is the heat lost by the room to the colder plenum [W]

Q_people is the sensible and latent (convective) heat generated by room occupants [W].

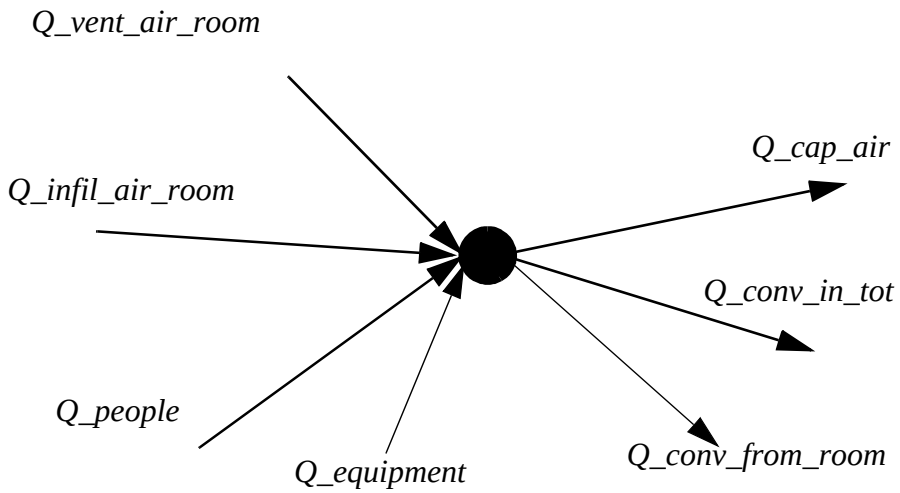

Figure A.24. Heat balance for the room air.

The heat balance is applied to a control volume with a boundary identical with the room envelope boundary. The SPARK algorithms used to calculate the heat terms in equation (A.99) are the following.

Q_cap_air_room

This term represents the heat stored in the room air:

$$Q_{cap-air-room} = \rho_{air} V_{room} c_{p-air} \frac{\partial T_{air-average}}{\partial t} \qquad \text{(A.100)}$$

where

$T_{air\_average}$ is the absolute temperature of the room air [K]

w_{room_air} is the room air humidity ratio [kg of vapor/ kg of dry air]

V_{room} is the room volume [m^3]

ρ_{room_air} is the room air density [kg/m^3], calculated as

$$\rho_{room-air} = \frac{0.62(1 + w_{room-air}) p_{air}}{287.5(0.62 + w_{room-air}) T_{air-average}} \qquad \text{(A.101)}$$

and

p_{air} is the air pressure inside the room [N/m^2]

c_{p_air} is the specific heat of the room air, [J/kg-K], calculated as (see [14]):

$$c_{p-air} = (1 - w_{room-air})c_{p-dry-air} + w_{room-air}c_{p-vapor} \quad \text{(A.102)}$$

where

$c_{p\_dry\_air}$ is the specific heat of dry air, considered constant and equal to 1006 J/kg-K

c_{p_vapor} is the specific heat of water vapor, considered constant and equal to 1805 J/kg-K.

Q_conv_in_tot

This term represents the heat lost by the room air to the room envelope, through convective heat transfer. The convective heat flux at each of the room surfaces is described in section A.4.3.1.

To conveniently use the fluxes (A.23), the convective heat in equation (A.99) is calculated as the sum of all the heat fluxes lost to all the wall surfaces (see section A.4.3.1), multiplied by the respective surface areas, plus the heat losses to the occupants and the equipment (including lights) in the room:

$$Q_{conv-in-tot} = \sum_i A_{in-i}q_{conv-in-i} + Q_{conv-occupants} + Q_{conv-equipment} \quad \text{(A.103)}$$

Q_vent_air_room

This term corresponds to the heat added to the room air by ventilation air (or air-conditioning, in the case of an all-air system). Considering that the density and pressure of the air is constant at a given moment, and neglecting the influences of differences in velocities and potential energy of the air flow domain, the ventilation heat term in the room air heat balance is expressed as [15]:

$$Q_{vent-air-room} = \dot{m}_{vent-air-flow}c_{p-air}(t_{inlet} - t_{air-average}) \quad \text{(A.104)}$$

where

$\dot{m}_{vent-air-flow}$ is the mass flow of the ventilation air [kg/s].

Q_infil_air_room

This term corresponds to the heat added to the room air by air infiltration. Based on the same assumptions as in the section about ventilation heat, the infiltration term in the

room heat balance is:

$$Q_{infil-air-room} = \dot{m}_{infil-air-flow} c_{p-air} (t_{air-out} - t_{air-average}) \qquad \text{(A.105)}$$

where

$\dot{m}_{infil-air-flow}$ is the mass flow of the infiltration air [kg/s].

It is generally difficult to obtain realistic infiltration data. Special computer programs, such as COMIS [16] address this problem in detail. Although several straightforward approaches have been found to estimate the air flow due to infiltration (see below), it is questionable whether the results obtained by using these approaches are accurate.

Infiltration air flow is proportional to the air change rate: this method assumes that the mass flow due to infiltration is proportional to the ventilation air flow. This is approach is very convenient because the air supplied by the ventilation system is generally known. However, this method fails for residential buildings.

DOE-2 Methodology: DOE-2 [6] users can select one of three different approaches to be used in the building simulation: no infiltration, the air change method, and the residential building method.

The "no infiltration" method ignores the influence of infiltration on the thermal balance of the building.

The "air change" method requires user input for the infiltration air flow. The infiltration air flow in this case is either constant, or corrected for the influence of wind speed near the building.

The "residential building" method considers that the infiltration air flow has a linear dependence of the wind speed near the building, and of the temperature difference between the interior and the exterior of the building. This method requires the user to provide the coefficients in the linear function.

From A Database: this method requires the program to access a database at each time step, provide data regarding the indoor and outdoor conditions, and extract the infiltration flow rates corresponding to those conditions. If the database has been obtained from calculations with programs designed especially for the modeling of infiltration (for example COMIS), this method can provide the most accurate results.

Due to the limitations of SPARK, the RADCOOL user must provide information regarding the infiltration air flow at each time step. Consequently, the user must specify the infiltration air flow as an input.

Q_conv_from_room

This term represents the heat transferred from the room to the plenum.

Consider the case where the room and plenum air have different temperatures. If the two spaces communicate, and if the room air is warmer than the plenum air, convection will cause mass and heat exchange between the room and the plenum. If the room air is colder than the plenum air, thermal stratification stops the mass and heat exchange.

This situation is analogous to Epstein's work on "air flow through horizontal openings" [17]. Epstein identifies four different regimes that depend on $\frac{L}{D}$, where L is the depth of the opening and D is the diameter of the opening.

In the case of a cooled panel, the opening area through which this air exchange takes place is the total "interstitial area" in the panel-covered ceiling. The existence of the interstitial area may be either due to the imperfect coverage of the ceiling with panels, or intentionally created by the system designer.

Consider a room with a 4 m x 5 m ceiling. The ceiling of the room could be covered with panels that are 20 cm thick and 5 m long. In this case the total crack length can be calculated as:

$$length_{crack} = \left(1 + \frac{width_{ceiling}}{width_{panel}}\right) length_{ceiling} = 105m \tag{A.106}$$

Assuming that the interstices are 3 mm wide, the total interstitial area is

$$area_{crack} = length_{crack} width_{crack} = 0.32m^2 \tag{A.107}$$

which gives a "lumped diameter"

$$D = \sqrt{\frac{4}{\pi} area_{crack}} = 0.63m \tag{A.108}$$

If the vertical depth of the crack is L = 1 cm (equal to the thickness of the panels), the ratio $\frac{L}{D}$ = 0.015. This corresponds to Epstein's Regime I, in which $\frac{L}{D}$ < 0.1. According to Epstein, this regime is governed by a Taylor instability in which the room air and panel air intrude into each other in the interstitial zone, leading to an oscillatory exchange. The regime is characterized by a constant dimensionless Froude number, and the air flow rate between the room and plenum depends only on the densities (or the temperatures) of the air in the room and plenum. According to Epstein, the fluid volume ratio in Regime I is:

$$\dot{V} = 0.04 D^{\frac{5}{2}} \left(g \frac{\Delta\rho}{\bar{\rho}}\right)^{\frac{1}{2}} \tag{A.109}$$

where

g is the acceleration due to gravity, 9.81 m/s^2

$\Delta\rho$ is the difference in density between the two fluids

$\bar{\rho}$ is the average density of the two fluids [kg/m^3].

Assuming that the fluid exchange takes place at constant pressure (a good approximation for the case of room-plenum air exchange), equation (A.109) is equivalent to

$$\dot{V} = 0.04 D^{\frac{5}{2}} \left(g \frac{-\Delta T}{\bar{T}} \right) \tag{A.110}$$

where

ΔT is the temperature difference between the room air and plenum air; the minus sign indicates that the flow occurs from the colder to the warmer zone.

$\bar{T}$ is the average between the room and plenum air temperatures.

Equation (A.110) can be used to determine the heat flow between the room and the plenum due to the air exchange, given by

$$Q_{conv-heat-from-room} = \rho_{air} \dot{V} c_{air} (T_{room} - T_{plenum}) \text{ if } T_{room} \geq T_{plenum} \text{ and}$$

$$Q_{conv-heat-from-room} = 0 \text{ if } T_{room} < T_{plenum}. \tag{A.111}$$

Q_people

This term represents the heat generated by the occupants in the room:

$$Q_{people} = Q_{sensible} + Q_{latent} + \{Respiration, Conduction, Transpiration\} \tag{A.112}$$

In equation (A.112), $Q_{sensible}$ and Q_{latent} are calculated as in DOE-2 [6]. The expression for $Q_{sensible}$ is:

$$Q_{sensible} = 0.293 \left\{ A_s + \left[B_s \left(\frac{9}{5} t_{dry-air} + 32 \right) \right] \right\} \tag{A.113}$$

where

$t_{dry\text{-}air}$ is the dry-bulb temperature of the room air (denoted so far by $t_{air\_average}$)

A_s and B_s are given by

$$A_s = 28 + 909.6 Q_m - 119.5 Q_m^2 \tag{A.114}$$

$$B_s = 1.2 - 100.48Q_m + 1.49Q_m^2 \quad \text{(A.115)}$$

and

Q_m is the heat gain due to the metabolic rate of the room occupants [W]:

$$Q_m = number_{occupants}\bar{A}_{occupant}(metabolic - rate) \quad \text{(A.116)}$$

In equation (A.116)

$A_{occupant}$ is the average body area given by the Dubois empirical equation:

$$\bar{A}_{occupant} = 0.203W^{0.425}H^{0.725} \quad \text{(A.117)}$$

where

W is the weight of the person [kg]

H is the height of the person [m].

The metabolic rate is usually expressed in *met* units (1 met = 58.15 W/m^2). The metabolic rate depends on the air temperature around a person, on the person's clothing and on the type of activity that the person performs [7].

The expression for Q_{latent} is:

$$Q_{latent} = 0.293\left\{A_l + \left[B_l\left(\frac{9}{5}t_{dry-air} + 32\right)\right]\right\} \quad \text{(A.118)}$$

with

$$A_l = 206 - 733.8Q_m + 160.9Q_m^2 \quad \text{(A.119)}$$

$$B_l = -6.7 + 15.16Q_m - 2.558Q_m^2 \quad \text{(A.120)}$$

Equations (A.113) and (A.118) give $Q_{sensible}$ and Q_{latent} in units of [W]. The respiration, conduction and transpiration terms in equation (A.112) are neglected in RADCOOL.

A.7.4 Plenum air heat balance

The plenum air interacts by convection with the back surface of the panel and with the ceiling surface. The plenum air can also be heated or cooled by the room air that enters the plenum. The heat balance for the plenum air is analogous to that for the room air (see Figure A.24):

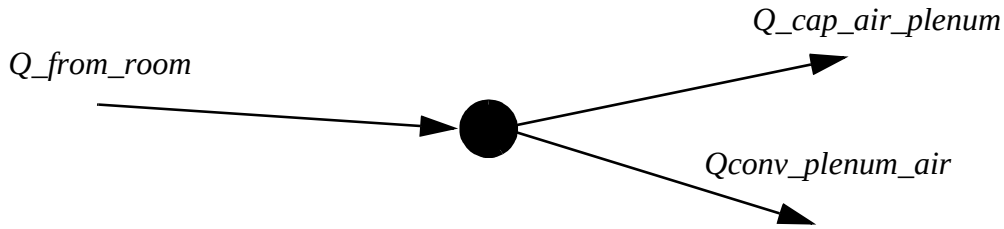

Figure A.25. Heat balance for the plenum air.

The heat balance equation for the plenum air is:

$$Q_{from-room} = Q_{cap-air-plenum} + Q_{conv-plenum-air} \quad \text{(A.121)}$$

where

Qcap_air_plenum is the heat stored in the plenum air as a result of the heat transfer [W]

Qconv_plenum_air is the total convective heat lost to the plenum surfaces [W]

Q_conv_from_room is the heat lost by the room to the colder plenum [W].

The heat balance is applied to a control volume whose boundary corresponds to the interior surfaces of the plenum. The algorithms to calculate the terms in equation (A.121) are similar to the ones described in section A.7.3.

The term representing the heat infiltrated from the room is the same (equations (A.106) - (A.111)).

In the case of the heat storage term, the only difference is that instead of room air quantities, equations (A.100) - (A.102) should be based on the specific heat, density, etc. corresponding to the plenum air.

The convection term in the plenum air balance can be calculated with the equation

$$Q_{conv-plenum-air} = \sum_i A_{in-i} q_{conv-in-i} \quad \text{(A.122)}$$

where the products in the right-hand side are calculated for all the surfaces inside the plenum.

A.7.5 Room air moisture balance

Moisture can be added to the room air by the supply air, the infiltration air, internal sources such as people, cooking, etc., and desorption from the internal surfaces of the room. Moisture leaves the room air in the exhaust air and through adsorption in the internal surfaces of the room. The balance equation for the room air humidity ratio, w_{room}, can be written as:

$$V_{room}\frac{dw_{room}}{dt} = \dot{v}_{vent}(w_{vent} - w_{room}) + \dot{v}_{infil}(w_{out} - w_{room}) + \frac{Q_{latent}}{\rho_{room}\lambda} + \frac{1}{\rho_{room}}W \qquad \text{(A.123)}$$

where

V_{room} is the room volume [m^3]

w_{room} is the room air humidity ratio [kg vapor/kg dry air]

$\dot{v}_{vent}$ is the ventilation air volume flow [m^3/s]

$\dot{v}_{infil}$ is the infiltration air volume flow [m^3/s]

w_{vent} is the ventilation air humidity ratio [kg vapor/kg dry air]

w_{out} is the outside air humidity ratio [kg vapor/kg dry air]

Q_{latent} is the latent heat production by people in the room [W], and can be calculated with equation (A.118)

ρ_{room} is the density of the room air [kg/m^3]

λ is the latent heat of vaporization for water [J/kg]

W is the rate of vapor adsorption/desorption on the walls [kg/s].

In RADCOOL, the rate of vapor adsorption/desorption is calculated based on the Cunningham theory of water sorption on building materials.

The main assumption in the Cunningham theory ([18] - [20]) is that the flux of water vapor through the surface of a wall is due to the difference in partial pressures between the wall material and the room air:

$$W = A_w h(p_w - p_{0w}) \tag{A.124}$$

where

A_w is the wall area involved in moisture exchange [m^2]

h is the moisture transfer coefficient under partial pressure forces [s/m]

p_w is the partial pressure of vapor inside the wall material [N/m^2]

p_{0w} is the partial pressure of vapor in the room air [N/m^2].

The moisture balance inside the wall material can be written as:

$$V_w \frac{dm_w}{dt} = -W \tag{A.125}$$

where

V_w is the wall volume involved in moisture exchange [m^3]

m is the mass of water found in the unit volume of wall material [kg/m^3].

It is obvious that equations (A.123) and (A.125) are coupled. Since there are no moisture sources inside a typical wall construction, the vapor sorption process is driven by the time variation of the moisture in the room air.

In practice, the humidity ratio of the room air can be roughly represented as having a cyclic variation with a given period (typically 24 h). The sorption process is therefore also periodic. Based on this observation, and on the slow character of moisture diffusion through a wall material, Cunningham [21] assumes that the wall volume involved in moisture exchange, V_w, represents only a small fraction of the wall volume. V_w can most conveniently be estimated using the "effective penetration depth theory" [22]. The effective penetration depth is defined as the wall depth reached by the moisture diffusion process under transient and cyclic conditions. V_w thus becomes:

$$V_w = d_{eff} A_w \tag{A.126}$$

where

d_{eff} is the effective penetration depth of the wall material [m].

Cunningham [21] shows that the effective penetration depth of a wall exposed to moisture variations on only one side can be calculated as:

$$d_{eff} = 2\sqrt{\frac{D_w}{2\omega}} = \sqrt{\frac{D_w T}{\pi}} \tag{A.127}$$

where

D_w is the water-vapor-in-wall-material diffusion coefficient [m^2/s]

ω is the frequency of variation of the room air humidity ratio [s^{-1}]

T is the period of variation of the room air humidity ratio (usually equal to 24 h) [s].

If the wall is exposed to moisture variation on both sides, the effective penetration depth is

$$d_{eff} = \frac{l}{3} \tag{A.128}$$

where

l is the thickness of the wall [m].

Generally, the sorption properties of building materials are communicated in the form of sorption curves. According to Cunningham [19] the sorption curves can be used in the calculation of W as follows. The partial pressure of vapor inside the wall material (see equation (A.124)) can be calculated as:

$$p_w = km \tag{A.129}$$

where

$$k = \frac{d(RH)}{d(MC)} \frac{p_{0w,\,sat}}{\rho_{wall}} \tag{A.130}$$

RH is the relative humidity of the room air [-]

MC is the moisture content of the wall material [kg water/kg dry wall material]

$d(RH)/d(MC)$ is the slope of the sorption curve [-]

$p_{0w,sat}$ is the saturation partial pressure of water vapor in the room air [N/m^2]

ρ_{wall} is the density of the wall material [kg/m^3]

and

$$m = (MC)\rho_{wall} \tag{A.131}$$

The partial pressure of water vapor in the room air (see equation (A.124)) can be calculated based on the relative humidity as:

$$p_{0w} = (RH)p_{0w,\,sat} \tag{A.132}$$

The substitution of equations (A.129) - (A.132) in (A.124) leads to the following expression for W:

$$W = A_w h\left[\frac{d(RH)}{d(MC)}(MC) - (RH)\right]p_{0w,\,sat} \tag{A.133}$$

By substituting equation (A.131) in the left-hand side of equation (A.125), the balance equation for the vapor content of the wall becomes:

$$V_w\frac{dMC}{dt} = -\frac{1}{\rho_{wall}}W \tag{A.134}$$

The sorption curves for a number of building materials are provided in [23]. These curves have the analytical form

$$ln(MC - MC_0) = A + Bln[(0.01RH)^{-c} - 1] \tag{A.135}$$

where

MC, MC_0 and *RH* are expressed as percentages

A, *B* and *c* are material-specific coefficients [-].

Equation (A.135) allows the calculation of the slope *d(RH)*/*d(MC)* as:

$$\frac{d(RH)}{d(MC)} = -\frac{100}{Bc}\times\frac{(0.01RH)^{-c-1}}{(0.01RH)^{-c}-1}\times\frac{1}{exp\{A + Bln[(0.01RH)^{-c}-1]\}} \tag{A.136}$$

Table A.1 contains the material-specific coefficients for some building materials.

Equation (A.130), expressing *k* as a function of the sorption curve slope, is correct in the approximation that the sorption curve is a line passing through the origin. For higher values of the *RH*, this approximation is obviously false. However, for high values of the *RH*, equation (A.130) can be replaced with:

$$k = \left(\frac{RH}{MC}\right)\frac{p_{0w,\,sat}}{\rho_{wall}} \tag{A.137}$$

TABLE A.1 Material-specific coefficients occurring in equation (A.136)[23].

Material	ρ [kg/m^3]	A	B	c	MC_0 [%]
Pine wood	530	2.97	-0.170	4.48	0
Hardboard	950	2.57	-0.160	4.50	0
Particle board	630	2.83	-0.195	3.50	0
Urea foam	10	3.31	-0.194	3.75	0
Fiberglass	17	1.59	-0.156	3.33	0
Asbestos cement	1310	2.03	-0.174	5.37	0
Concrete block	1580	0.841	-0.195	3.24	0
Brick	2020	1.02	-0.256	2.28	0
Limestone	1590	-1.21	-0.305	1.37	0
Gypsum plaster	740	1.784	-0.0492	7.134	8.65
Fibrous plaster	850	2.140	-0.0437	7.529	16.47

where the fraction *RH*/*MC* can be calculated using equation (A.135):

$$\frac{RH}{MC} = \frac{RH}{exp\{A + Bln[(0.01RH)^{-c} - 1]\}} \tag{A.138}$$

Where *RH* is expressed in %.

RH/*MC* as expressed in (A.138) is only a function of *RH*, and is therefore straightforward to calculate for a given *RH* if the coefficients *A*, *B* and *c* of the sorption curve are known.

The coefficient of moisture transfer under partial pressure forces in equations (A.124) and (A.133) is defined as:

$$h = \frac{h_m}{\frac{RT_{air,\,room}}{M_{vapor}}} \tag{A.139}$$

where

R is the universal gas constant [J/kmol-K]

$T_{air,room}$ is the absolute room air temperature [K]

M_w is the molecular weight of water vapor [kg/kmol]

h_m is the mass transport coefficient under concentration gradient forces [m/s].

According to the Lewis theory of convection, h_m can be calculated as:

$$h_m = \frac{h_{conv}}{\rho_{air} c_{p,\,air} (Le)^{\frac{2}{3}}} \tag{A.140}$$

where

h_{conv} is the convection film coefficient [W/m^2-K]

$c_{p,air}$ is the specific heat of air under constant pressure [J/kg-K]

Le is the Lewis number of air

$$Le = \frac{\alpha}{D} \tag{A.141}$$

α is the air heat diffusion coefficient [m^2/s]

D is the water-vapor-in-air diffusion coefficient [m^2/s].

As an example, for air at 25 °C and a convection coefficient of 3.25 W/m^2-K, h_m is 3.03x10^{-3} m/s, and *h* is 2.2x10^{-8} s/m.

The diffusion coefficient can be calculated based on the vapor permeability of the wall material. The permeability is defined as:

$$\mu = -\frac{g}{\frac{dP}{dx}} \tag{A.142}$$

where

μ is the permeability of the material [kg/m-s-Pa] = [s]

g is the mass flux of water into the material [kg/m^2-s]

P is the partial vapor pressure inside the material [N/m^2]

x is the distance inside the material where P is measured [m].

Based on the permeability of the material, the material water-vapor-diffusion coefficient can be calculated [24] as:

$$D_w = \mu \frac{p_{0w,\,sat}}{\rho_{wall} \frac{d(MC)}{d(RH)}} \tag{A.143}$$

Introducing (A.130) in (A.143) leads to

$$D_w = \mu k \tag{A.144}$$

Tviet [25] measured the variation in permeability due to changes in the relative humidity of the room air. The permeability variation with relative humidity can be expressed as:

$$\mu = exp(f_0 + f_1 RH + f_2 RH^2) \tag{A.145}$$

where f_0, f_1 and f_2 are material-specific coefficients (see Table A.2).

TABLE A.2 Material-specific coefficients occurring in equation (A.145) [25].

Material	f_0	f_1	f_2
Pine wood	-28.71886	-0.1194911	4.158788
Hardboard	-26.62005	-0.3730495	1.386730
Particle board	-25.32247	0.0357264	0.781466
Urea foam	-23.72120	0.9761170	-0.2620779
Fiberglass	-22.67872	0.	0.
Asbestos cement	-25.35854	-0.2456131	1.526852
Concrete block	-27.78411	-0.1738898	1.451546
Brick	-24.98131	0.	0.
Limestone	-26.12126	0.0790142	0.9812424
Gypsum plaster	-26.08942	-0.3126156	2.503194
Fibrous plaster	-26.72177	0.7450913	0.5223077

Table A.3 contains the permeability, diffusion coefficient and effective penetration depth for different materials. The data corresponds to a *RH* of 50% and an air temperature of 25 °C. Data referring to the permeability curves of materials can also be found in [26].

Thomas and Burch [27] present experimental data regarding the moisture content of two building materials, and computer simulation efforts to model the results of their asymptotic-type experiments.

In order to evaluate the model presented in this section, an effort was made to simulate the results obtained by Thomas and Burch in their experiments. During the process of modeling, however, it became clear that the effective penetration depth theory is appropriate for asymptotic-type experiments only if the calculated effective depth is equal to, or larger than the material thickness. In the cases where this condition does not apply, a multiple-node model is necessary.

TABLE A.3 Permeability, diffusion coefficient, and effective penetration depth of different materials [25].

Material	μ [10^{12} kg/m-s-Pa]	k [m^2/s^2]	D_w [10^{10} m^2/s]	d_{eff} [10^3 m]
Pine wood	0.898	32.3	0.29	0.89
Hardboard	3.22	27.7	0.89	1.56
Particle board	12.5	31.2	3.90	3.27
Urea foam	76.1	1204.3	916.4	50.2
Fiberglass	141.0	4642.9	6546.5	134.1
Asbestos cement	12.5	31.7	3.96	3.30
Concrete block	1.13	92.9	1.05	1.70
Brick	14.1	54.4	7.67	4.59
Limestone	6.01	564.3	33.91	9.66
Gypsum plaster	7.47	129.7	9.69	5.16
Fibrous plaster	4.11	83.1	3.41	3.06

The multiple-node model can be formulated similarly to the Thomas and Burch model [27]. For a two-node model, the balance equations are:

$$V_{eff}\frac{dMC_{eff}}{dt} + \frac{1}{\rho_{wall}}W_{eff} = \frac{1}{\rho_{wall}}W_{deep} \tag{A.146}$$

and

$$V_{deep}\frac{dMC_{deep}}{dt} = -\frac{1}{\rho_{wall}}W_{deep} \tag{A.147}$$

where

V_{eff} is the volume of the effective layer, given by (A.126) [m^3]

V_{deep} is the volume of the material less the volume of the effective layer [m^3]

W_{eff} is the flux of water vapor leaving the material, described by (A.133) [kg/s]

W_{deep} is a similar flux of water vapor, occurring inside the material [kg/s].

$$W_{deep} = \rho_w A_w D_w \frac{MC_{deep} - MC_{eff}}{d_{deep}} \tag{A.148}$$

and

d_{deep} is the thickness of the material less the thickness of the effective layer [m].

It is obvious that for $d_{deep} \rightarrow \infty$, $d_{eff} \rightarrow d_{material}$, $W_{deep} \rightarrow 0$, and (A.146) becomes (A.134).

In the present version, RADCOOL performs air moisture calculations based on the two-node model for the wall (equations (A.146)-(A.147)), and on the moisture balance described in equation (A.123).

A.8 Linking Objects

The class of components entitled “linking objects” is composed of the objects that connect the other classes of components together. In the present version of RADCOOL there are four types of linking objects:

- the total convective heat for the air heat balance (equation (A.103))
- the air temperatures in the vicinity of the room surfaces (equations (A.94) - (A.98))
- the total short wave radiation entering the room through transparent surfaces (equation (A.44)), and
- the long wave radiation between the interior room surfaces (equations (A.41) - (A.43)).

It is obvious that the specific content and size of each of the linking objects depend on the number of surfaces defined in a particular room. The SPARK programs corresponding to these linking objects must be “customized” to fit each particular situation. For this reason, the SPARK programs corresponding to linking must be created in the preliminary data processing phase of RADCOOL. However, once created, these linking programs can be saved in the SPARK library, and can be reused whenever a new situation occurs that involves a room layout similar to a situation already examined in the past.

A.9 Tasks Performed in the “Preliminary Data Processing” Section

A.9.1 Data collection

The first task performed in the “preliminary data processing” section is the acquisition of information about the building to be modeled. At the end of this task, the collected data should provide a unique description of the building to be modeled.

Relevant data include:

- the characteristics of the building: number, type (passive, radiant), and position of walls, number and position of windows, types and positions of floors, etc.
- the characteristics of the building site: location and orientation of the building, and weather information (solar radiation, outside air temperature, ground temperature, wind, etc.)
- occupancy and equipment schedules: number of occupants, types of activities performed, equipment installed in the building, etc.
- the air flow characteristics (ventilation flow rate and supply temperature, infiltration flow rate)
- the HVAC system characteristics (thermostat setpoints, etc.)
- the quantities that the user desires as a result of the calculation.

After this information has been collected, the user must convert it into input for the SPARK program. Some data, such as the thermal properties of building materials, the hourly weather data, etc. may be available in databases. Other data, such as shape factors and weather-dependent thermal properties, must be calculated. The remainder of this section will describe the procedures presently used in RADCOOL to calculate shape factors and weather-related inputs.

A.9.2 Weather-related data

Weather-related quantities that are required as input include primary weather data (such as ambient drybulb and dew-point temperatures), soil temperature, and cloud cover. These quantities can usually be found in the weather file corresponding to a particular site. Other weather-related data must be calculated. These data include:

- the outside surface convective film coefficient h_{conv_out} of each exterior wall; h_{conv_out} depends on the outside temperature, the exterior surface temperature, the wind speed and direction, etc.; in RADCOOL this value is currently obtained by performing a DOE-2 calculation at the same location and printing the DOE-2 hourly output for the convection film coefficient.
- the sky emissivity ε_{sky},which depends on the outside air dew-point temperature and on the sky cover (equation (A.25)).
- the direct and diffuse solar radiation incident on each exterior surface, which depend on the position of the Sun, on cloud cover, and on the orientation of the surface; in RADCOOL these values are currently obtained from DOE-2 hourly output.

• the solar absorptivity of each glazing layer, and the overall solar transmittance of each window, which depend on the glazing type, the window orientation, and the position of the Sun; in RADCOOL these values are currently obtained from DOE-2 hourly output.

In order to offer an idea about the complexity of the weather-related calculations, the next section describes the algorithm used in DOE-2 for the calculation of the direct and solar radiation incident on an exterior surface.

A.9.2.1 Algorithms to calculate the direct and diffuse solar radiation on a surface

Among other quantities, a typical weather file includes the following hourly measured data: direct normal solar radiation, diffuse horizontal solar radiation, and global horizontal solar radiation. As stated in section A.4.3.3, in order to perform a heat balance calculation for an exterior surface, the user must supply information about the direct and diffuse solar radiation incident on the surface. The following algorithms describe the calculations performed to obtain the direct and diffuse solar radiation incident on a surface with an arbitrary orientation from the data supplied by a typical weather file. These algorithms are used in DOE-2, and are based on [28].

Weather file quantities

The values used in the calculation are the direct normal solar radiation, I_{DN}, and the total horizontal solar radiation, I_{tH}, as reported in the typical weather file.

Solar position-related quantities

The calculation of direct and diffuse irradiance on a surface with an arbitrary orientation requires inputs related to the following sun-related quantities: the apparent solar time and the solar angles with respect to the given surface.

a. Apparent solar time

The apparent solar time depends on the local civil time, the geographical position of the building site, and the fluctuations in the velocity of the Earth [28], according to

$$AST = LST + ET + 4(LSM - LON) \qquad \text{(A.149)}$$

where

AST is the apparent solar time [hours]

LST is the local standard time [hours]

ET is the value of the equation of time for the day of the year when the calculation is made [hours]

LSM is the local standard time meridian [degrees of an arc]

LON is the local longitude [degrees of an arc]

4 is the number of minutes it takes the Earth to rotate 1° of an arc.

According to [6], ET can be developed in a Fourier series as a function of the day of the year, *n*:

$$ET = A_0 + A_1 \cos W + A_2 \cos 2W + A_3 \cos 3W + B_1 \sin W + B_2 \sin 2W + B_3 \sin 3W \tag{A.150}$$

with

$$W = \left(\frac{2\pi}{365}\right) n \tag{A.151}$$

The coefficients in (A.151) are given in Table A.4.

TABLE A.4 Coefficients for equation (A.150) [6].

A_0	A_1	A_2	A_3	B_1	B_2	B_3
0.000696	0.00706	-0.0533	-0.00157	-0.122	-0.156	-0.00556

b. Solar angles

The position of the sun with respect to the site is usually described by the solar altitude β, and solar azimuth ϕ, measured from the south. The solar azimuth is positive for afternoon hours and negative for morning hours. Both these angles depend on the solar declination δ, the hour angle *H*, and the latitude *L*, according to:

$$\sin\beta = \cos L \cos\delta \cos H + \sin H \sin\delta \tag{A.152}$$

$$\cos\phi = \frac{\sin\beta \sin L - \sin\delta}{\cos\beta \cos L} \tag{A.153}$$

Consider a surface with azimuth Ψ measured from south and a tilt angle Σ. The surface solar azimuth γ, is defined as:

$$\gamma = \phi - \Psi \tag{A.154}$$

If $90° < \gamma < 270°$, the surface is in shadow.

The angle of incidence ϑ, of direct radiation on the surface is defined as the angle between the normal to the surface and the ray from the surface to the sun. The angle ϑ is given by

$$\cos\vartheta = \cos\beta\cos\gamma\sin\Sigma + \sin\beta\cos\Sigma \qquad \text{(A.155)}$$

Direct solar radiation incident on a surface with an arbitrary orientation

The direct solar radiation I_D, incident on a surface depends on the direct normal solar radiation, I_{DN}, and on the angle of incidence, ϑ:

$$I_D = I_{DN}\cos\vartheta, \text{ if } \cos\vartheta > 0$$

$$I_D = 0, \text{ if } \cos\vartheta \le 0 \qquad \text{(A.156)}$$

Diffuse solar radiation incident on a surface with an arbitrary orientation

The diffuse solar radiation, I_d, is the sum of diffuse ground-reflected radiation, I_{dg}, and diffuse sky radiation, I_{ds}.

$$I_d = I_{dg} + I_{ds} \qquad \text{(A.157)}$$

A simple expression for I_{ds} is

$$I_{ds} = CI_{DN}F_{sky} \qquad \text{(A.158)}$$

where

F_{sky} is the sky form factor (A.26), with $\Phi_{wall} = \Sigma$.

Similarly, I_{dg} is given by

$$I_{dg} = I_{th}\rho_g F_{ground} \qquad \text{(A.159)}$$

where

ρ_g is the ground reflectance

F_{ground} is the ground form factor (A.29), with $\Phi_{wall} = \Sigma$.

In equations (A.158) and (A.159) C is the sky diffusion factor:

$$C = A_0 + A_1\cos W + A_2\cos 2W + A_3\cos 3W + B_1\sin W + B_2\sin 2W + B_3\sin 3W \qquad \text{(A.160)}$$

with W calculated as in equation (A.151).

The coefficients in (A.160) are given in Table A.5.

TABLE A.5 Coefficients for equation (A.160) [6].

A_0	A_1	A_2	A_3	B_1	B_2	B_3
0.0905	-0.041	0.0073	0.0015	-0.0034	0.0004	-0.0006

For vertical surfaces, it is possible to express the diffuse radiation in terms of the total horizontal solar radiation, I_{tH}:

$$I_d = YI_{tH} \tag{A.161}$$

where the factor Y can be written as:

$$Y = 0.55 + 0.437\cos\vartheta + 0.313(\cos\vartheta)^2 \qquad \text{if } \cos(\vartheta) > -0.2$$

$$Y = 0.45 \qquad \text{if } \cos\vartheta \le -0.2 \tag{A.162}$$

A.9.3 Surface-to-surface shape factors

As stated in section A.4.4.2, every surface in an enclosure exchanges long wave (IR) radiation with the other surfaces in the enclosure. The net long wave radiation absorbed by surface *i* in an *N*-surface enclosure is given by equations (A.41) - (A.43). This section describes the calculation of the shape factors F_{ij}.

The shape factor F_{ij} between surface *i* and surface *j* represents the fraction of the total long wave radiation emitted by surface *i* that is incident on surface *j*. In an *N*-surface enclosure, the shape factors depend only on the geometry of the surfaces. The general equation for F_{ij} for surfaces *i* and *j* having the areas A_i and A_j respectively, is [9]:

$$F_{ij} = \frac{1}{A_i}\int_{A_i}\int_{A_j}\frac{\cos\theta_i\cos\theta_j}{\pi S^2}dA_i dA_j \tag{A.163}$$

where

S is the distance between a point on i and a point on j

θ_i is the angle between the normal on surface *i* and the line connecting surfaces *i* and *j*

θ_j is the angle between the normal on surface *j* and the line connecting surfaces *i* and *j*.

The integral in the right hand side of (A.163) is not always easy to calculate. In the case of rectangular surfaces, the shape factors can be calculated through shape factor algebra. Shape factor algebra provides relationships between analytically calculated shape factors corresponding to a given relative position of two surfaces, and shape factors corresponding to another given relative position of two surfaces [9].

The simplest relative positions in which two rectangular surfaces can be found in a building are (see Figure A.26)

- parallel to each other, and
- making a 90° angle with each other.

Solving equation (A.163) for these two relative positions yields exact solutions for the shape factors F_{12} and F_{21}. For example, in the case of two walls making a 90° angle, F_{12} can be calculated as [9]:

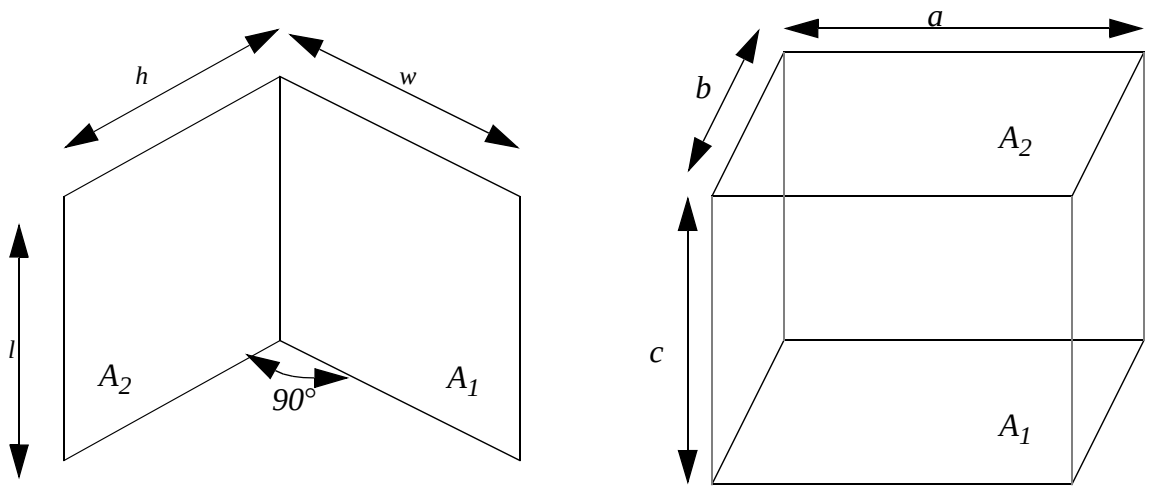

Figure A.26. Relative positions of two rectangular surfaces that give exact solutions for the shape factors.

$$F_{12} = \frac{1}{\pi W}(term_1 - term_2) \qquad \text{(A.164)}$$

where

$$term_1 = W\operatorname{atan}\frac{1}{W} + H\operatorname{atan}\frac{1}{H} - \sqrt{H^2 + W^2}\operatorname{atan}\frac{1}{\sqrt{H^2 + W^2}} \tag{A.165}$$

$$term_2 = \frac{1}{4}ln\left\{\frac{(1 + W^2)(1 + H^2)}{1 + W^2 + H^2}term_3\right\} \tag{A.166}$$

$$term_3 = \left[\frac{W^2(1 + W^2 + H^2)}{(1 + W^2)(W^2 + H^2)}\right]^{W^2}\left[\frac{H^2(1 + H^2 + W^2)}{(1 + H^2)(H^2 + W^2)}\right]^{H^2} \tag{A.167}$$

$$H = \frac{h}{l} \tag{A.168}$$

$$W = \frac{w}{l} \tag{A.169}$$

In the case of two parallel walls, F_{12} can be calculated as:

$$F_{12} = \frac{2}{\pi XY}(term_4 + term_5) \tag{A.170}$$

where

$$term_4 = ln\left[\frac{(1 + X^2)(1 + Y^2)}{1 + X^2 + Y^2}\right]^{\frac{1}{2}} - X\operatorname{atan}X - Y\operatorname{atan}Y \tag{A.171}$$

$$term_5 = X\sqrt{1 + Y^2}\operatorname{atan}\frac{X}{\sqrt{1 + Y^2}} + Y\sqrt{1 + X^2}\operatorname{atan}\frac{Y}{\sqrt{1 + X^2}} \tag{A.172}$$

$$X = \frac{a}{b} \tag{A.173}$$

$$Y = \frac{c}{b} \tag{A.174}$$

Once the shape factor F_{12} has been calculated, F_{21} can be calculated by using the basic relationship of shape factor algebra:

$$F_{ji} = \frac{A_i}{A_j}F_{ij} \tag{A.175}$$

Another useful relationship of shape factor algebra describes the long wave radiation exchange between two surfaces when one of the surfaces is subdivided in two or more sub-surfaces (see Figure A.27).

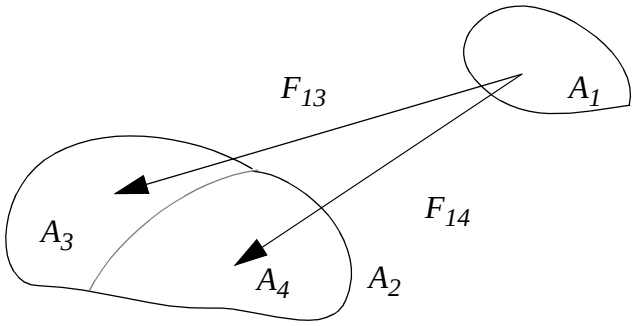

Figure A.27. Radiation exchange between finite areas with one area subdivided.

Consider an arbitrary area A_1 exchanging radiation with a second area A_2. The shape factor F_{12} is the fraction of the total radiation emitted by A_1 that is incident on A_2. If A_2 is divided into two parts, A_3 and A_4, the fraction of the total energy leaving A_1 that is incident on A_3 and the fraction of the total energy leaving A_1 that is incident on A_4 must add up to F_{12}. Therefore

$$F_{12} = F_{13} + F_{14} \tag{A.176}$$

To calculate the shape factors between arbitrarily located rectangles, both integration and shape factor algebra are necessary.

In RADCOOL, the shape factor calculations are performed by using a TRNSYS subroutine [29]. The TRNSYS subroutine calculates shape factors for all the surfaces that form an enclosure. The input information required by this subroutine refers to the relative positioning of the surfaces inside the enclosure.

A.10 References

1. Edward F. Sowell, W. F. Buhl, A. E. Erdem, and F. C. Winkelmann, *A prototype object-based system for HVAC simulation*. Proc. Second Int. Conf. System Simulation in Buildings, Liège, Belgium, 1986. Rep. LBNL-22106.

2. Fred Buhl, E. Erdem, J.-M. Nataf, F. C. Winkelmann, M. Moshier and E. Sowell, *Advances in SPARK*. Proc. Third Int. Conf. System Simulation in Buildings, Liège, Belgium, 1994. Rep. LBNL-29419.

3. H. S. Carslaw and J. C. Jaeger, *Conduction of heat in solids*. Clarendon Press, Second edition, Oxford, 1978.

4. Joseph H. Klems, *U-Values, solar heat gain and thermal performance: recent studies using the MoWiTT*. Rep. LBL-25487, 1989. Revised, Mo-254.

5. *TARP Reference manual*. NBSIR 83-2655, 1981.

6. Simulation Research Group (LBL) and Group Q-11 (LANL), *DOE-2 Engineering manual*. Rep. LBNL-11353, 1982.

7. P. O. Fanger, *Thermal comfort*. McGraw-Hill, New York, 1970.

8. B. F. Raber and F. W. Hutchinson, *Panel heating and cooling analysis*. John Wiley, New York, 1947.

9. R. Siegel and J. R. Howell, *Thermal radiation heat transfer*. Second Edition, Hemisphere Publishing Corporation, 1981.

10. Jack P. Holman, *Heat transfer*. Seventh Edition, McGraw-Hill, New York, 1990.

11. Frank P. Incropera and D. P. Dewitt, *Fundamentals of heat and mass transfer - third edition*. New York: Wiley, 1990.

12. R. W. Shoemaker, *Radiant heating*. McGraw-Hill, Second Edition, New York, 1954.

13. C. Q. Chen and J. Van der Kooi, *Accuracy - a program for combined problems of energy analysis, indoor air flow and air quality*. ASHRAE Trans. (94) 1988.

14. R. Brandemuehl, S. Gabel, and I. Andresen, *A toolkit for secondary HVAC system energy calculations*. Prepared for ASHRAE, University of Colorado at Boulder, 1993.

15. H. D. Baehr, *Thermodynamik*. 7th Edition, Springer Verlag, 1989.

16. Helmut E. Feustel and A. Rayner-Hooson, Ed., *COMIS Fundamentals*. Rep. LBNL-28560, 1990.

17. M. Epstein, *Buoyancy-driven exchange flow through small openings in horizontal partitions*. Trans. of the ASME, Journal of Heat Transfer, (110) 1988.

18. M. J. Cunningham, *A new analytical approach to the long term behavior of moisture concentrations in building cavities - I. Non-condensing cavity*. Building and Environment, (18) (3) 1983.

19. M. J. Cunningham, *Further analytical studies of building cavity moisture concentrations*. Building and Environment, (19) (1) 1984.

20. M. J. Cunningham, *The moisture performance of framed structures - a mathematical model*. Building and Environment, (23) (2) 1988.

21. M. J. Cunningham, *Effective penetration depth and effective resistance in moisture transfer*. Building and Environment, (27) (3) 1992.

22. A. Keresteciogl̈u, M. Swami and A. Kamel, *Theoretical and computational investigation of simultaneous heat and moisture transfer in buildings: "effective penetration depth" theory*. ASHRAE Trans., (96) (1) 1990.

23. M. J. Cunningham and T.J. Sprott, *Sorption properties of New Zealand building materials*. Research Report R43, Building Research Association of New Zealand, Judgeford, 1984.

24. D. M. Burch, W.C. Thomas and A.H. Fanney, *Water vapor permeability measurements of common building materials*. ASHRAE Transactions, (98) (2) 1992.

25. A. Tviet, *1966 Measurements of moisture sorption and moisture permeability of porous materials*. Rep. Norwegian Building Research Institute - 45, Oslo, 1966.

26. R. R. Zarr, D.M. Burch and A.H. Fanney, *Heat and moisture transfer in wood-based wall construction: measured versus predicted*. NIST Building Science Series 173, 1995.

27. W. C. Thomas and D.M. Burch, *Experimental validation of a mathematical model for predicting water vapor sorption at interior building surfaces*. ASHRAE Transactions, (96) (1) 1990.

28. ASHRAE Handbook, *Fundamentals*. American Society for Heating, Refrigeration and Air-Conditioning Engineers, Inc., Atlanta, 1993.

29. Solar Energy Laboratory, *TRNSYS, a transient simulation program. Reference manual*. University of Wisconsin, Madison, 1994.